The Plant Cell, Vol. 19: 1809–1825, June 2007, www.plantcell.org

BLADE-ON-PETIOLE1 and *2* Control *Arabidopsis* Lateral Organ Fate through Regulation of LOB Domain and Adaxial-Abaxial Polarity Genes [W]

Chan Man Ha,[a,b,c] Ji Hyung Jun,[a,b,c] Hong Gil Nam,[b] and Jennifer C. Fletcher[a,c,1]

[a] Plant Gene Expression Center, U.S. Department of Agriculture/University of California Berkeley, Albany, California 94710
[b] Division of Molecular Life Science and the I-BIO Graduate Program, Pohang University of Science and Technology San 31, Hyoja-dong Pohang, Kyungbuk 790-784, Korea
[c] Department of Plant and Microbial Biology, University of California, Berkeley, California 94720

We report a novel function for *BLADE-ON-PETIOLE1* (*BOP1*) and *BOP2* in regulating *Arabidopsis thaliana* lateral organ cell fate and polarity, through the analysis of loss-of-function mutants and transgenic plants that ectopically express *BOP1* or *BOP2*. *35S:BOP1* and *35S:BOP2* plants exhibit a very short and compact stature, hyponastic leaves, and downward-orienting siliques. We show that the *LATERAL ORGAN BOUNDARIES* (*LOB*) domain genes *ASYMMETRIC LEAVES2* (*AS2*) and *LOB* are upregulated in *35S:BOP* and downregulated in *bop* mutant plants. Ectopic expression of *BOP1* or *BOP2* also results in repression of class I *knox* gene expression. We further demonstrate a role for *BOP1* and *BOP2* in establishing the adaxial-abaxial polarity axis in the leaf petiole, where they regulate *PHB* and *FIL* expression and overlap in function with *AS1* and *AS2*. Interestingly, during this study, we found that *KANADI1* (*KAN1*) and *KAN2* act to promote adaxial organ identity in addition to their well-known role in promoting abaxial organ identity. Our data indicate that *BOP1* and *BOP2* act in cells adjacent to the lateral organ boundary to repress genes that confer meristem cell fate and induce genes that promote lateral organ fate and polarity, thereby restricting the developmental potential of the organ-forming cells and facilitating their differentiation.

INTRODUCTION

Continuous lateral organ formation is critical for higher plants to produce their characteristic architectures, but the regulatory pathways that specify organ cell fate are still poorly understood. In angiosperms, leaves are derived from small populations of founder cells set aside on the flanks of the pluripotent shoot apical meristem (SAM). These leaf primordia are separated from the main shoot through the establishment of a boundary between the organ-forming cells and the meristem cells that provides a permissive environment for differentiation. Once leaf primordia initiate, leaves grow rapidly through active cell division and expansion from the initial primordia cells into mature organs with three developmental axes of polarity: the proximodistal, the dorsoventral (adaxial-abaxial), and mediolateral axes (Waites and Hudson, 1995).

A number of mutants displaying leaf formation defects have been isolated in *Arabidopsis thaliana*. Plants carrying a mutation in either *ASYMMETRIC LEAVES1* (*AS1*) or *AS2* form asymmetric, rumpled, lobed leaves with ectopic leaflet-like organs on the petioles (Tsukaya and Uchimiya, 1997; Serrano-Cartagena et al., 1999; Byrne et al., 2000; Ori et al., 2000; Semiarti et al., 2001; Sun et al., 2002). *AS1* encodes a MYB domain–containing putative transcription factor (Byrne et al., 2000) and is closely related to *PHANTASTICA* (*PHAN*) in *Antirrhinum majus* and *ROUGH SHEATH2* in *Zea mays* (Waites et al., 1998; Timmermans et al., 1999; Tsiantis et al., 1999). *AS2* encodes a widely expressed protein with a Leu zipper motif (Iwakawa et al., 2002; Xu et al., 2002). Genetic studies have revealed that *AS1* and *AS2* function in overlapping developmental pathways (Serrano-Cartagena et al., 1999; Ori et al., 2000; Semiarti et al., 2001). Moreover, the AS1 and AS2 proteins interact in yeast two-hybrid assays (Xu et al., 2003). Both genes act in the leaves to repress the expression of three class I *knox* genes, *BREVIPEDICELLUS* (*BP*), *KNAT2*, and *KNAT6*, which promote the activity and maintenance of the SAM (Byrne et al., 2000; Ori et al., 2000; Semiarti et al., 2001). Leaf initiation occurs via a reciprocal negative molecular interaction between class I *knox* genes and *AS1* and *AS2*: the class I *knox* gene *SHOOT MERISTEMLESS* negatively regulates *AS1* and *AS2* expression in the SAM, while *AS1* and *AS2* in turn repress *BP*, *KNAT2*, and *KNAT6* activity in the initiating primordia (Byrne et al., 2000, 2002).

AS2 is a member of the plant-specific *LATERAL ORGAN BOUNDARIES* (*LOB*) domain (LBD) family of proteins (Iwakawa et al., 2002; Shuai et al., 2002; Xu et al., 2002). *LOB*, the founding *LBD* family member, is expressed at the boundary between the SAM and developing organ primordia (Shuai et al., 2002) and is positively regulated by *AS1* and *AS2* (Byrne et al., 2002; Shuai

[1] To whom correspondence should be addressed. E-mail fletcher@nature.berkeley.edu; fax 510-559-5678.
The author responsible for distribution of materials integral to the findings presented in this article in accordance with the policy described in the Instructions for Authors (www.plantcell.org) is: Jennifer C. Fletcher (fletcher@nature.berkeley.edu).
[W] Online version contains Web-only data.
www.plantcell.org/cgi/doi/10.1105/tpc.107.051938

et al., 2002). *lob* plants show no developmental defects, most likely because of functional redundancy between *LOB* and other *LBD* genes. However, plants that ectopically express *LOB* are dwarfed and produce small leaves that curl upward slightly at the margins (Shuai et al., 2002). Ectopic expression of the *LBD* gene *LBD36/ASL1* (Iwakawa et al., 2002; Shuai et al., 2002) also causes the formation of upward-curling (hyponastic) leaves and downward-pointing siliques (Nakazawa et al., 2003; Chalfun-Junior et al., 2005). Like *lob* plants, loss-of-function *lbd36/asl1* plants do not display detectable mutant phenotypes, but *AS2* and *LBD36/ASL1* have overlapping functions during flower formation (Chalfun-Junior et al., 2005).

Following leaf initiation, a number of *Arabidopsis* genes act to specify leaf polarity along the adaxial-abaxial axis. Five members of the class III homeodomain/Leu zipper (HD-ZIP) family of transcription factors specify adaxial organ identity (McConnell and Barton, 1998; McConnell et al., 2001; Emery et al., 2003; Prigge et al., 2005). Their mRNAs are targeted by two microRNAs, miR165 and miR166, leading to their downregulation in abaxial cells (Tang et al., 2003; Bao et al., 2004; Kim et al., 2005; Williams et al., 2005). Conversely, *KANADI* (*KAN*) gene family members, along with *YABBY* (*YAB*) gene family members, confer abaxial identity and growth (Eshed et al., 1999; Sawa et al., 1999; Siegfried et al., 1999; Kerstetter et al., 2001; Emery et al., 2003; Eshed and Bowman, 2004). *35S:AS2* transgenic plants form nearly radial, adaxialized leaves (Lin et al., 2003; Xu et al., 2003) and *as2* alleles in the Landsberg *erecta* (L*er*) background condition the appearance of abaxial cellular morphology in the adaxial region of leaves (Xu et al., 2003). Ectopic *AS2* expression leads to upregulation of *PHABULOSA* (*PHB*), a class III *HD-ZIP* gene, and to repression of *KAN1*, *KAN2*, and the *YAB* genes *FILAMENTOUS FLOWER* (*FIL*) and *YAB3* (Lin et al., 2003).

Arabidopsis as1 leaves show only weakly abaxialized characteristics in contrast with orthologous *Antirrhinum phan* leaves that are severely abaxialized, suggesting the presence of redundant factors in the *AS1-AS2* pathway. Recently, several genes were reported as genetic enhancers of the *as1* or *as2* polarity phenotype. Combinations between *as1* or *as2* and mutations in genes that function in *trans*-acting short-interfering RNA production, for example, *RNA-DEPENDENT RNA POLYMERASE6*, *SUPPRESSOR OF GENE SILENCING3*, *ARGONAUTE7*, and *DICER-LIKE4*, result in severely enhanced adaxial/abaxial polarity defects (Li et al., 2005; Adenot et al., 2006; Fahlgren et al., 2006; Garcia et al., 2006; Xu et al., 2006). Furthermore, mutations in the subunits of the 26S proteasome, such as *AE3* (*RPN8a*), strongly enhance the polarity defects of *as1* or *as2* leaves (Huang et al., 2006). These data suggest that organ polarity specification is controlled at the transcriptional, posttranscriptional, and post-translational levels.

Like *AS2* and *AS1*, the *Arabidopsis BLADE-ON-PETIOLE1* (*BOP1*) gene plays an important role in suppressing meristematic activity in developing lateral organ primordia through the repression of class I *knox* gene expression (Ha et al., 2003). *BOP1* acts synergistically with *AS1* and *AS2* to regulate leaf morphogenesis (Ha et al., 2003). *BOP1* and *BOP2* encode closely related BTB/POZ domain and ankyrin repeat–containing proteins that have largely overlapping expression patterns (Ha et al., 2004; Hepworth et al., 2005; Norberg et al., 2005). In this study, we report the phenotypic and molecular effects of *BOP1* and *BOP2* null alleles and overexpression lines in wild-type and various leaf mutant backgrounds. We demonstrate that *BOP1* and *BOP2* positively regulate the expression of *AS2* and *LOB* and that *BOP* overexpression leads to upregulation of *LBD36/ASL1*. Conversely, high levels of *BOP1* and *BOP2* expression cause downregulation of the class I *knox* genes *BP*, *KNAT2*, and *KNAT6*. We show that *bop1 bop2* leaf petioles exhibit abaxialized vasculature, a defect that is enhanced in the *as1* or *as2* backgrounds, and that changes in *BOP1* and *BOP2* activity alter the expression of the organ polarity genes *PHAVOLUTA* (*PHV*) and *FIL*. Finally, we find that *KAN1* and *KAN2* function in the establishment of adaxial and abaxial organ identity.

RESULTS

BOP1 and *BOP2* Have Overlapping Functions during Development

BOP1 and *BOP2* are closely related genes with very similar transcription patterns, which are largely restricted to the base of developing lateral organs (Ha et al., 2004; Hepworth et al., 2005; Norberg et al., 2005). To reveal the full spectrum of *BOP* function in *Arabidopsis* plants, we isolated *bop1* and *bop2* null alleles and generated double mutants. The *bop1-4* null allele was reported previously (Ha et al., 2003, 2004). Since *bop2* null alleles had not been previously identified, we characterized a new *BOP2* insertion allele, *bop2-11*. This allele contains a T-DNA insertion at nucleotide +1414 in the second exon within the sequence encoding the ankyrin repeats. We could not detect full-length *BOP2* transcripts in *bop2-11* plants (see Supplemental Figure 1 online).

BOP1 and *BOP2* have overlapping functions in leaf organogenesis. Compared with wild-type Columbia (Col-0) plants (see Supplemental Figure 2A online), *bop1-4* plants developed a single ectopic outgrowths from the leaf petiole region with low penetrance (see Supplemental Figure 2B online). By contrast, *bop2-11* plants showed normal rosette leaf morphogenesis (see Supplemental Figure 2C and Supplemental Table 1 online). Interestingly, *bop1-4 bop2-11* double mutant plants developed extensive ectopic blade outgrowths along the rosette leaf petiole, like those observed in homozygous *bop1-1* plants (see Supplemental Figure 2D online; Ha et al., 2003), revealing a synergistic genetic interaction between *BOP1* and *BOP2*. Cauline leaves of *bop1* but not *bop2* plants frequently developed ectopic outgrowths from the basal region (see Supplemental Figures 2F and 2G online), while *bop1-4 bop2-11* plants displayed an enhanced cauline leaf outgrowth phenotype (see Supplemental Figure 2H online) compared with *bop1-4* plants. These data indicate that *BOP1* and *BOP2* function in a redundant pathway to suppress excess growth in proximal positions during leaf development.

Both *bop1* and *bop2* plants displayed defects in inflorescence development. *bop2-11* plants frequently formed fused and/or fasciated inflorescences and generated multiple flowers from the same node (see Supplemental Figure 2J and Supplemental Table 1 online). These defects were rarely detected either in wild-type or in *bop1* plants (see Supplemental Figure 2I and Supplemental Table 1 online). *bop1-4 bop2-11* inflorescences

displayed slightly enhanced phenotypes compared with those of either single mutant (see Supplemental Figure 2K and Supplemental Table 1 online; Hepworth et al., 2005; Norberg et al., 2005). As reported previously (Hepworth et al., 2005; Norberg et al., 2005), we found that *BOP1* and *BOP2* act redundantly during reproductive development to control bract suppression, floral patterning, and floral organ number (data not shown). In addition, we observed a novel defect in gynoecium formation: whereas the gynoecium of wild-type flowers consists of two fused carpels (see Supplemental Figure 2L online), ~50% of *bop1-4 bop2-11* gynoecia contained only a single, fertile carpel (see Supplemental Figure 2M online). These data indicate additional functional redundancy between *BOP1* and *BOP2* in regulating aspects of inflorescence and flower development.

Ectopic Expression of *BOP1* and *BOP2*

To further investigate the function of *BOP1* and *BOP2* in plant development, we generated transgenic plants that ectopically expressed either *BOP1* or *BOP2* under the control of the constitutive 35S promoter. Transformation of the *35S:BOP1* construct into *bop1-4 bop2-11* plants rescued the mutant phenotypes, indicating that this construct is functional in vivo (data not shown).

One-third (90/251) of transgenic plants containing *35S:BOP1* in the L*er* background displayed significant developmental defects that could be categorized into four classes. Class I plants (22/251) were the most severely affected. They displayed a small, compact overall shape, rounded rosette leaves with short petioles, strongly hyponastic rosette leaves, severely reduced stem elongation, and densely packed clusters of flowers with little

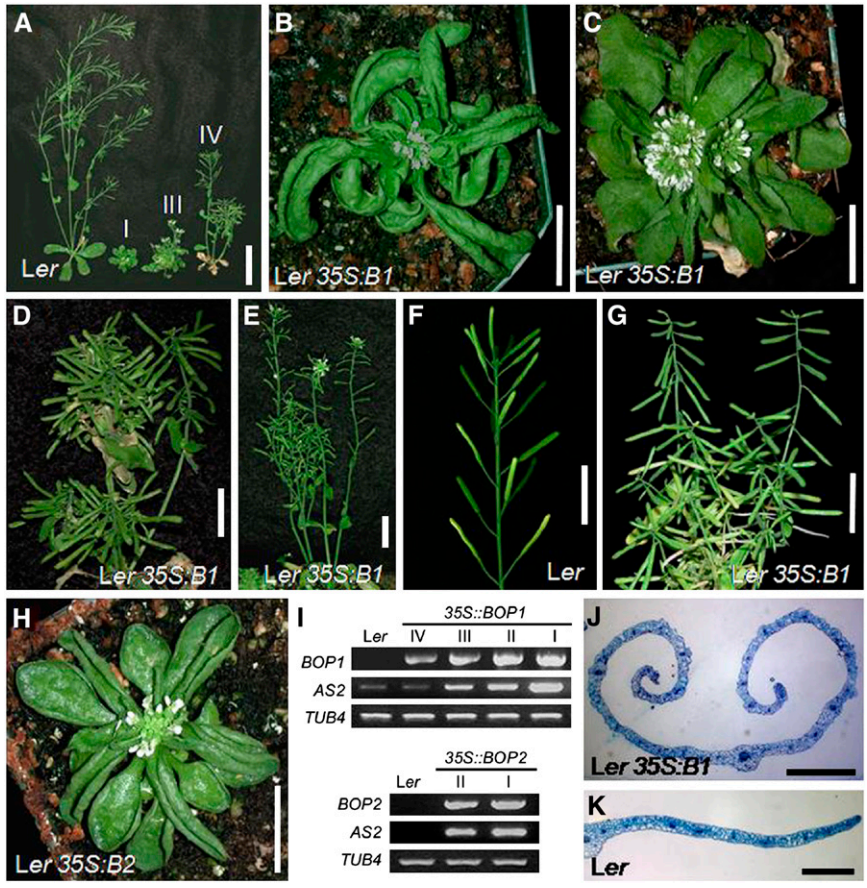

Figure 1. Phenotypes of *BOP1* and *BOP2* Overexpressor Plants.

(A) Phenotypic variation among *35S:BOP1* (*35S:B1*) plants. From left to right: L*er* wild-type (L*er*), *35S:BOP1* class I (I), class III (III), and class IV (IV) transgenic plants.
(B) to **(E)** Class I **(B)**, class II **(C)**, class III **(D)**, and class IV **(E)** *35S:BOP1* transgenic plants.
(F) and **(G)** Inflorescence development in L*er* wild-type **(F)** and *35S:BOP1* **(G)** plants.
(H) *35S:BOP2* transgenic plant (*35S:B2*).
(I) *BOP1*, *BOP2*, and *AS2* expression in *35S:BOP1* and *35S:BOP2* plants. RNA was isolated from the leaves of 35-d-old *35S:BOP1* T1 plants displaying class I, class II, class III, or class IV phenotypes or from 35-d-old *35S:BOP2* T1 plants displaying class I or class II phenotypes. *TUBULIN4* (*TUB4*) was used as a control.
(J) and **(K)** Cross section through a *35S:BOP1* **(J)** and a L*er* **(K)** leaf.
Bars = 40 mm in **(A)**, 10 mm in **(B)** to **(H)**, and 1 mm in **(J)** and **(K)**.

internode growth (Figures 1A and 1B, Table 1). These plants produced small numbers of aborted seeds. Class II plants (20/251) displayed all of the phenotypes exhibited by class I plants but had a weak hyponastic leaf character (Figure 1C, Table 1). Class III plants (25/251) developed normal-sized rosettes and leaves but had a strong clustering of flowers with reduced growth of the inflorescence shoot (Figure 1D, Table 1). Class IV plants (23/251) had nearly normal leaf and shoot growth but either displayed a weak clustering of flowers and slightly reduced shoot growth or were indistinguishable from wild-type plants except that their siliques developed in abnormal orientations (Figure 1E, Table 1). More than 80% of class III and >50% of class IV plants also exhibited weak hyponastic leaf morphology. Wild-type plants formed upward-orienting siliques (Figure 1F). By contrast, although class I and class II plants formed shoot apices that were too compact to determine silique orientation, class III and class IV shoots formed siliques that grew sharply downward and/or outward at abnormal angles (Figure 1G, Table 1). The severity of the abnormal silique orientation phenotype was stronger in class III plants than class IV plants. The overall severity of the *35S:BOP1* phenotypes correlated with the level of *BOP1* transcription, as *BOP1* expression was highest in class I plants and lowest in class IV plants (Figure 1I).

We also examined the effects of ectopic *BOP2* expression. Transformation of the *35S:BOP2* construct into *bop1-4 bop2-11* plants rescued the mutant leaf development phenotype (data not shown). Ectopic expression of *BOP2* in the L*er* background caused a range of developmental phenotypes similar to those observed in *35S:BOP1* transgenic plants (Figure 1H, Table 1). As observed for *35S:BOP1*, the phenotypic severity of *35S:BOP2* transgenic plants correlated with the level of *BOP2* transcription (Figure 1I).

To further examine the morphological defects in *35S:BOP1* plants, we examined the internal cellular structure of the rosette leaves from class I plants. Strong hyponastic leaf morphology was clearly observed in transverse sections through *35S:BOP1* leaves (Figures 1J and 1K). However, we were unable to detect a specific difference in the arrangement of vasculature and mesophyll cells along the adaxial-abaxial axis, or in epidermal cell morphology on either the adaxial or the abaxial surface, of *35S:BOP1* rosette leaves compared with those of wild-type plants.

BOP1 and *BOP2* Negatively Regulate Class I *knox* Gene Expression

We have previously shown that several class I *knox* genes were misexpressed in semidominant *bop1-1* mutant leaves (Ha et al., 2003). To further explore the role of *BOP1* and *BOP2* in class I *knox* gene regulation, we examined *BP*, *KNAT2*, and *KNAT6* expression in *bop1* and *bop2* loss-of-function and overexpressing plants. The expression levels of *BP*, *KNAT2*, and *KNAT6* were relatively unaffected in *bop1-4* and *bop2-11* seedlings compared with wild-type Col seedlings but were significantly increased in *bop1-4 bop2-11* seedlings (Figure 2A). *KNAT2* and *KNAT6* transcript levels were relatively unaltered in *BOP1* and *BOP2* overexpressor plants compared with wild-type L*er* plants. However, *BP* mRNA levels were reduced in the shoots of 25-d-old *35S:BOP1* and *35S:BOP2* plants (Figure 2B). *35S:BOP1* and *35S:BOP2* plants displayed a downward-growing silique phenotype similar to that of *bp* mutant plants (Douglas et al., 2002; Venglat et al., 2002). *BP* expression was strongly reduced in the stems of *BOP* transgenic plants compared with those of wild-type plants (Figure 2C), suggesting that the downward-orienting silique phenotype of *35S:BOP1* and *35S:BOP2* plants is caused by a severe decrease in *BP* activity.

The *erecta* Mutation Conditions Severe *BOP1* Overexpressor Phenotypes

The phenotypic defects of our *35S:BOP1* plants were considerably more severe than those previously reported (Norberg et al., 2005). A likely explanation for this is the difference in the genetic backgrounds used in the two analyses, since the prior study used the Col ecotype, whereas we used the L*er* ecotype. The *erecta* (*er*) mutation is known to influence leaf polarity because the asymmetric leaf differentiation in the adaxial/abaxial axis of *as2-101* plants is dependent on the presence of *er* (Xu et al., 2003). To determine the potential contribution of *er* to the appearance of *35S:BOP1* phenotypes, we transformed the *35S:BOP1* construct

Table 1. Phenotypes of *BOP1* and *BOP2* Overexpressor Lines (%)

						Downward Silique	
Transgenic Line (T1)	Total[a]	Class I	Class II	Class III[b]	Class IV[b]	Strong[c]	Weak[d]
L*er 35S:BOP1*	251	8.8	8.0	10.0 (84)	9.2 (52)	3.2	11.6
L*er 35S:BOP2*	117	10.3	11.1	12.8 (87)	13.7 (31)	4.3	12.8
Lan *35S:BOP1*	180	0	2.8	4.4 (0)	8.3 (0)	0.0	0.6
as2-101 35S:BOP1	122	0	8.2	11.5 (0)	13.1 (0)	0.8	16.4
as1-101 35S:BOP1	66	0	12.1	10.6 (0)	13.6 (0)	0.0	13.6
lob 35S:BOP1	190	15.8	4.7	6.8 (92)	5.8 (36)	6.8	9.5
lob 35S:BOP2	183	13.1	4.4	12.6 (96)	13.1 (38)	8.2	13.7

[a] Number of T1 plants examined.
[b] Numbers in parenthesis denote the percentage of plants with weakly upward curling morphology among class III and class IV plants, respectively.
[c] Strongly downward-orienting siliques.
[d] Weakly downward-orienting siliques, including those developing at abnormal angles.

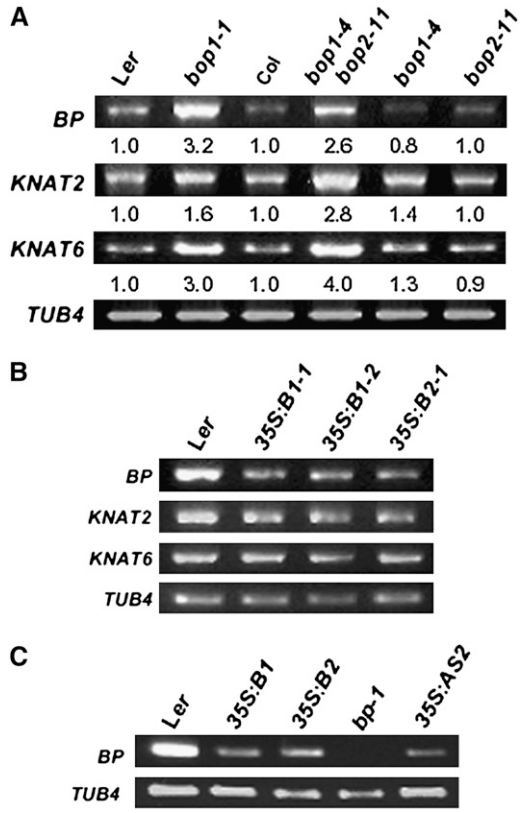

Figure 2. Expression of Class I *knox* Genes.

(A) RT-PCR analysis of class I *knox* gene expression using RNA isolated from the shoot region of 12-d-old seedlings. The relative amount of transcript accumulation in the various genotypes is indicated below each image.

(B) RT-PCR analysis of class I *knox* gene expression using RNA isolated from the shoot region of 25-d-old plants. *35S:B1-1*, *35S:B1-2*, and *35S:B2-1* represent independent transgenic lines.

(C) RT-PCR analysis of *BP* expression in the stem region. *TUB4* was used as a control.

into Landsberg (Lan) plants that are wild-type at the *ER* locus. We could not detect class I plants among Lan *35S:BOP1* transformants (Table 1), and the percentage of class II, class III, and class IV plants was decreased in Lan *35S:BOP1* plants compared with L*er 35S:BOP1* plants. Furthermore, upward-curling leaf development was not detected in any class of Lan *35S:BOP1* transformants (Table 1). Thus, these data indicate that the *er* mutation is required for the appearance of the severe phenotypic defects in L*er 35S:BOP1* plants.

BOP1 and *BOP2* Positively Regulate *LBD* Gene Expression

Ectopic expression of either *AS2* or *LOB* has been shown to cause phenotypic defects, such as hyponastic leaf development (Shuai et al., 2002; Xu et al., 2003), similar to those observed in *35S:BOP1* and *35S:BOP2* plants. Thus, one interpretation of our results is that the phenotypic defects observed in the *BOP1* and *BOP2* overexpression lines are caused by increased *AS2* and/or *LOB* expression. To test this hypothesis, we examined the transcript levels of both genes in the *BOP* overexpression lines. Expression levels of both *AS2* and *LOB* were highly upregulated in *35S:BOP1* and *35S:BOP2* plants (Figure 3A). Moreover, the elevated *AS2* expression level in *35S:BOP1* and *35S:BOP2* plants was correlated with the phenotypic severity of the transgenic plants, with plants displaying the strongest phenotypes also exhibiting the highest levels of *AS2* transcripts (Figure 1I). Conversely, *LOB* expression was decreased in *bop1-1* and *bop1-4 bop2-11* plants, especially strongly in the *bop1-1* dominant-negative

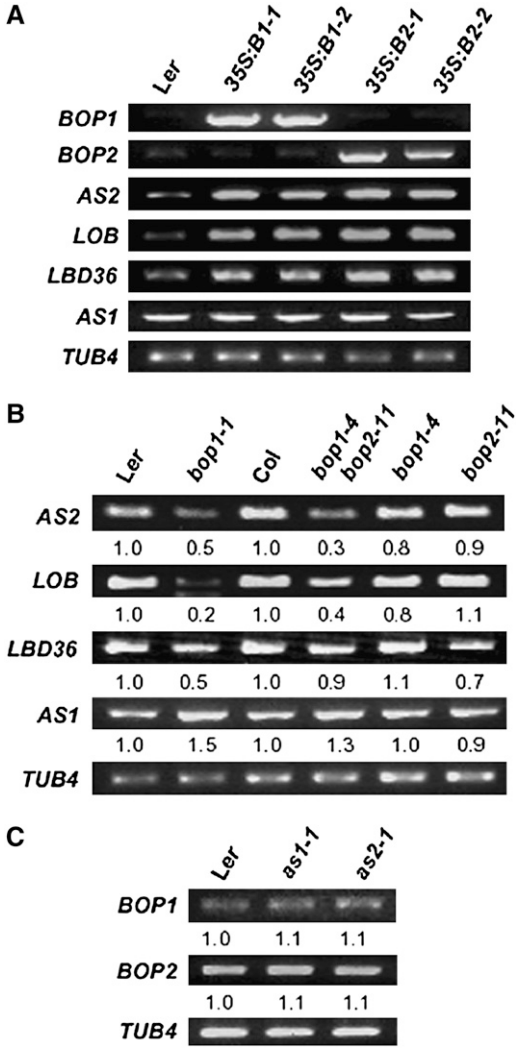

Figure 3. Expression of *AS1* and *LOB* Domain Genes.

(A) RT-PCR analysis of *BOP*, *AS1*, and *LOB* domain gene expression in *35S:BOP* plants. RNA was isolated from the shoots of 15-d-old plants. *35S:B1-1*, *35S:B1-2*, *35S:B2-1*, and *35S:B2-2* represent independent transgenic lines.

(B) RT-PCR analysis of *AS1* and *LBD* gene expression in *bop* plants. RNA was isolated from the shoots of 12-d-old plants.

(C) RT-PCR analysis of *BOP1* and *BOP2* expression in 12-d-old *as1* and *as2* plants. The relative amount of transcript accumulation in the various genotypes is indicated below each image. *TUB4* was used as a control.

mutant background (Figure 3B). *AS2* transcript levels were also reduced in *bop1-1* and *bop1-4 bop2-11* plants. Taken together, these results indicate that *BOP1* and *BOP2* are necessary and sufficient to induce high-level expression of *AS2* and *LOB*.

LBD36/ASL1 encodes a LOB domain protein with the highest sequence similarity to AS2 (Iwakawa et al., 2002; Shuai et al., 2002), with which it has overlapping functions in the flower (Chalfun-Junior et al., 2005). Misexpression of *LBD36/ASL1* resulted in a hyponastic leaf phenotype (Chalfun-Junior et al., 2005) like that observed in *BOP1* and *BOP2* overexpression lines. We found that *LBD36/ASL1* transcript levels were elevated in *35S:BOP1* and *35S:BOP2* plants (Figure 3A) and were reduced in *bop1-1* but not *bop1-4 bop2-11* plants (Figure 3B). Thus, we conclude that *BOP1* and *BOP2* can also upregulate *LBD36/ASL1* when they are ectopically expressed.

AS1 has overlapping functions with AS2 in regulating leaf morphogenesis and interacts with the AS2 protein. In contrast with *AS2* and the other two *LOB* domain genes, *AS1* expression levels were unchanged in both *35S:BOP1* and *35S:BOP2* plants. However, *AS1* transcript levels were slightly elevated in *bop1-1* and *bop1-4 bop2-11* plants compared with the wild type. *AS1* is expressed in the initiating leaf primordia region (Byrne et al., 2000), and *bop* mutant plants develop many ectopic leaf primordia along the petiole. We therefore interpret these results to indicate that the increased level of *AS1* transcription in *bop* mutant plants might be derived not from negative regulation by *BOP1* and *BOP2* but from its induction in the ectopic leaf primordia formed on *bop* mutant leaves. We detected no change in *BOP1* or *BOP2* expression levels in *as1* and *as2* mutant plants compared with wild-type plants (Figure 3C); thus, neither *AS1* nor *AS2* is required for the activation of the *BOP* genes.

Neither *AS2* transcripts nor *LOB* transcripts have been detected in seedling tissues using in situ hybridization, but a *LOB* enhancer trap line (*lob:ET22*) with an (ET):β-glucuronidase (GUS) reporter gene insertion in the 3′ end of the *LOB* gene exists that allows examination of *LOB* transcriptional activity via GUS assay (Shuai et al., 2002). These *lob* mutant plants do not show any detectable phenotypes, likely because of redundancy with other *LBD* family genes (Shuai et al., 2002). To observe the spatial effect of *BOP1* and *BOP2* activity on *LOB* expression, we crossed plants carrying the *lob:ET22* GUS reporter construct to *bop1-1* and *bop1-4 bop2-11* plants and also transformed the *35S:BOP1* construct into *lob:ET22* plants.

In *lob* plants, the *lob:ET22* enhancer trap drove GUS reporter gene expression at the shoot apex, in the hypocotyl, at the base of all lateral organs, and in the roots (Figure 4A; Shuai et al., 2002). In *bop1-1* plants containing *lob:ET22*, we could not detect GUS gene activity in the shoot apex (Figure 4B). In *bop1-4 bop2-11* plants containing *lob:ET22*, GUS expression was observed in the shoot apex but more weakly than in *lob* plants (cf. Figures 4A and 4C). Conversely, ectopic expression of *BOP1* resulted in increased and expanded *lob:ET22* GUS expression in the shoot apex (Figure 4D). We also detected ectopic GUS activity broadly across the blade region of *35S:BOP1* leaves (Figure 4D, arrows), a pattern that was not observed in *lob* leaves. In *lob* flowers, *LOB* GUS activity was detected in the anthers and at the base of siliques and pedicels, respectively (Figure 4E; Shuai et al., 2002). In *bop1-1* and *bop1-4 bop2-11* flowers, GUS expression from *lob:ET22* was also observed in these organs but

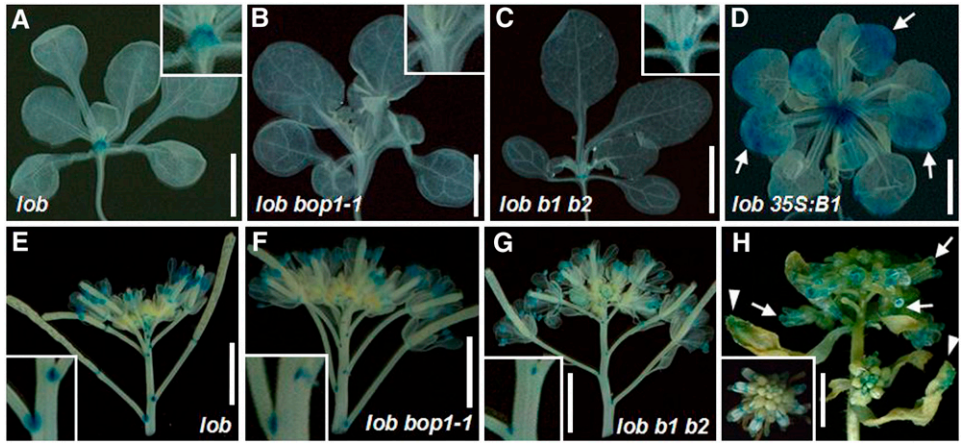

Figure 4. Expression Analysis of GUS Activity in a *lob* Enhancer Trap Line.

(A) to **(C)** *lob* **(A)**, *bop1-1* **(B)**, and *bop1-4 bop2-11* **(C)** seedlings carrying a *lob:ET22* enhancer trap construct, showing GUS expression at the shoot apex of each plant. Insets show a higher magnification of the shoot apex in each plant.

(D) *35S:BOP1* seedling carrying a *lob:ET22* enhancer trap construct, showing extensive GUS expression around the SAM. Arrows indicate ectopic GUS expression in the leaf blades.

(E) to **(G)** *lob* **(E)**, *bop1-1* **(F)**, and *bop1-4 bop2-11* **(G)** inflorescences carrying a *lob:ET22* enhancer trap construct, showing GUS expression in the anthers, the abscission zone, and the base of the pedicels. Insets show a higher magnification of the base of the pedicels in each plant.

(H) *35S:BOP1* inflorescence carrying a *lob:ET22* enhancer trap construct, showing GUS expression in the anthers, the abscission zone, and the base of the pedicels. GUS expression is also detected ectopically in the stigmatic tissue (arrows) and cauline leaves (arrowheads). Inset shows a top view. Bars = 5 mm.

more weakly than in *lob* flowers (Figures 4F and 4G). In the flowers of *35S:BOP1* plants, GUS activity was detected in the wild-type expression domain and also ectopically in the stigmatic tissues at the tip of the gynoecia (Figure 4H, arrows) and at the distal end of cauline leaves (Figure 4H, arrowheads). Thus, ectopic *BOP1* activity is sufficient to induce ectopic *LOB* transcription outside the context of its normal expression domain in both leaves and flowers.

35S:BOP1 Phenotypes Require *AS2* and *AS1* but Not *LOB*

Previous genetic and molecular analyses indicated that *BOP1* and *AS2* act in overlapping developmental pathways (Ha et al., 2003). *35S:BOP1* and *35S:BOP2* transgenic plants display a similar range of phenotypes as *35S:AS2* plants, and *AS2* is strongly upregulated in *35S:BOP1* and *35S:BOP2* plants. These observations suggested that *AS2* might be required to condition the phenotypes of *35S:BOP1* and *35S:BOP2* transgenic plants.

To test this hypothesis, we transformed the *35S:BOP1* construct into *as2-101* plants. The *as2-101* allele was derived from ethyl methanesulfonate–treated L*er* plants, and plants carrying this allele displayed weak phenotypes (Figure 5A; Xu et al., 2002). *as2-101 35S:BOP1* plants displayed the same short stature and reduced internode elongation as L*er 35S:BOP1* plants, and their siliques were pointed outward or slightly downward (Figures 5B and 5C, Table 1). However, the strongly downward-orienting silique phenotype observed in L*er 35S:BOP1* plants was very rarely detected in *as2-101 35S:BOP1* plants (Figure 5C, Table 1). We also could not find plants with strongly upward-curling leaf morphology among the *as2-101 35S:BOP1* plants (Table 1). In addition, weakly upward-curling leaves were not detected among class III and class IV *as2-101 35S:BOP1* plants, although they were readily observed in class III and class IV L*er 35S:BOP1* plants. Conversely, when the *35S:AS2* construct was transformed into *bop1-1* plants, none of the 175 T1 transgenic plants showed rescue of the *bop1-1* leaf phenotypes (data not shown).

Molecular, genetic, and biochemical data indicate that *AS1* and *AS2* act together in leaf development (Serrano-Cartagena et al., 1999; Ori et al., 2000; Semiarti et al., 2001; Byrne et al., 2002; Xu et al., 2003). To determine whether *AS1* is required for the *35S:BOP1* phenotypes, we transformed the *35S:BOP1* construct into the weak *as1-101* allele in the L*er* background (Figure 5D; Sun et al., 2002; Xu et al., 2003). *as1-101 35S:BOP1* plants exhibited a similar range of phenotypes as L*er 35S:BOP1* plants (Figures 5E and 5F, Table 1). However, in *as1-101 35S:BOP1* plants, strongly upward-curling leaves were not detected and siliques developed at abnormal angles rather than in a strongly downward orientation (Figure 5F, Table 1). Thus, both *AS1* and *AS2* are required to condition the *35S:BOP1* leaf morphology and silique orientation phenotypes.

AS1 and *AS2* positively regulate the expression of *LOB* (Byrne et al., 2002; Shuai et al., 2002), and we have shown here that *LOB* is also positively regulated by *BOP1* and *BOP2*. To determine whether *LOB* is required for the acquisition of the *BOP1* and *BOP2* overexpression phenotypes, the *35S:BOP1* and *35S:BOP2* constructs were introduced into *lob:ET22* mutant plants (Figure 5G). *lob 35S:BOP1* and *lob 35S:BOP2* plants exhibited identical phenotypes to L*er 35S:BOP1* and L*er 35S:BOP2* plants, both with respect to the range of phenotypes and to the ratio of each phenotypic class (Figures 5H and 5I, Table 1). The number of plants with the class I hyponastic leaf shape was even slightly increased in *lob 35S:BOP1* and *lob 35S:BOP2* plants compared with L*er 35S:BOP1* and L*er 35S:BOP2* plants. Taken together, these results indicate that *LOB* activity is not necessary to condition the *35S:BOP1* and *35S:BOP2* phenotypes.

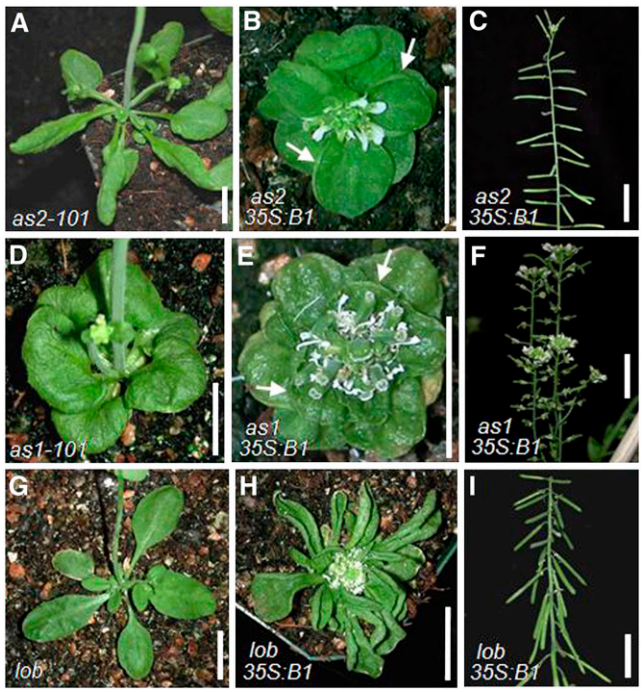

Figure 5. Effects of *BOP1* Overexpression in Leaf Mutants.

(A), **(D)**, and **(G)** Forty-day-old *as2-101* **(A)**, *as1-101* **(D)**, and *lob* plants **(G)**.
(B), **(E)**, and **(H)** Forty-day-old *as2-101 35S:BOP1* **(B)**, *as1-101 35S:BOP1* **(E)**, and *lob 35S:BOP1* plants **(H)**. Arrows in **(B)** and **(E)** indicate weak upward-curling leaf morphology.
(C), **(F)**, and **(I)** Inflorescences of *as2-101 35S:BOP1* **(C)**, *as1-101 35S:BOP1* **(F)**, and *lob 35S:BOP1* plants **(I)**.
Bars = 10 mm.

Genetic Interaction between *bop1 bop2* and Organ Polarity Mutants

The *bop1 bop2* leaf phenotypes are reminiscent of those of *as1* or *as2* plants, which form lobed and rumpled leaves (Figures 6A, 6B, 6G, and 6H; Tsukaya and Uchimiya, 1997; Serrano-Cartagena et al., 1999; Byrne et al., 2000; Ori et al., 2000; Semiarti et al., 2001; Sun et al., 2002). In addition, we have determined that *AS2* is positively regulated by *BOP1* and *BOP2* and that *AS1* and *AS2* function is required for the appearance of many *35S:BOP1* phenotypes. These data suggested that *BOP1* and *BOP2* might play roles in leaf morphogenesis events mediated by *AS1* and *AS2*.

We investigated this possibility by examining the phenotypic effects of combining the *bop1-4 bop2-11* alleles with severe *as1-1* or *as2-1* alleles. The rosette leaf petioles of *bop1 bop2 as1*

Figure 6. Genetic Interaction between *bop1 bop2* Mutants and Organ Polarity Mutants.

(A), **(B)**, **(G)**, and **(H)** Forty-day-old *as2-1* (**[A]** and **[B]**) and *as1-1* plants (**[G]** and **[H]**).
(C), **(D)**, **(I)**, and **(J)** Forty-five-day-old *bop1 bop2 as2-1* (**[C]** and **[D]**) and *bop1 bop2 as1-1* plants (**[I]** and **[J]**).
(E), **(F)**, **(K)**, and **(L)** Forty-eight-day-old *kan1 kan2 as2-15* (**[E]** and **[F]**) and *kan1 kan2 as1-1* plants (**[K]**) and **[L]**).
(B), **(D)**, **(F)**, **(H)**, **(J)**, and **(L)** each show a detached single rosette leaf.
(M) to **(O)** Forty-five-day-old *kan1 kan2* plants **(M)** and *bop1 bop2 kan1 kan2* plants (**[N]** and **[O]**). **(O)** shows a detached rosette leaf.
(P) to **(R)** Detached rosette leaf from *bop1 bop2* introgressed once into L*er* (x1L) plants **(P)**, *kan1 kan2* **(Q)**, and *bop1 bop2 kan1 kan2* plants **(R)**. Left images show the adaxial view, while right images show the abaxial view. In **(Q)** and **(R)**, insets show ectopic blade outgrowths on the abaxial side of the rosette leaf.
(S) Detached radialized leaves of *bop1 bop2 kan1 kan2* plants.
Arrows in **(D)**, **(J)**, **(N)**, and **(O)** indicate ectopically developed radialized leaves. r, rosette leaf; el, ectopic leaf; *b1 b2*, *bop1 bop2*; *k1 k2*, *kan1 kan2*. Bars = 10 mm.

and *bop1 bop2 as2* plants showed extensive ectopic outgrowth formation in the marginal region (Figures 6C, 6D, 6I, and 6J), and some outgrowths exhibited a strongly radialized character (Figures 6D and 6J, arrows). To identify the origin of these ectopic organ outgrowths, we performed anatomical analysis of young seedlings. The leaf petioles of 11-d-old Col, *as1-1*, and *as2-1* seedlings were fully differentiated and consisted of highly vacuolated cells lacking a detectable nucleus (see Supplemental Figures 3A to 3C online). By contrast, *bop1 bop2*, *bop1 bop2 as1*, and *bop1 bop2 as2* leaf petioles displayed clusters of densely cytoplasmic, undifferentiated cells on the adaxial side, coincident with the development of ectopic outgrowths (see Supplemental Figures 3D to 3F online, arrows). These data show that the double and triple mutant leaf petioles acquired ectopic meristematic activity in the adaxial regions.

To further characterize the *bop1 bop2*, *bop1 bop2 as1*, and *bop1 bop2 as2* phenotypes, we analyzed the internal morphology of the leaf petioles. The petioles of wild-type leaves contain polarized vascular bundles consisting of xylem on the adaxial side and phloem on the abaxial side (Figures 7A and 7G). Interestingly, some *bop1 bop2* leaf petioles (22.2%) had xylem surrounded by phloem (Figures 7B and 7H, Table 2), which is characteristic of the abaxialized lateral organs produced by *Antirrhinum phan* plants and by *Arabidopsis phb phv rev* and *as2 enhancer3* (*ae3*) plants (Waites and Hudson, 1995; Emery et al., 2003; Huang et al., 2006). More than 55% of *bop1 bop2* petioles formed half-moon-shaped vasculature, with xylem developing on the inside and phloem on the outside. We interpret this as partially abaxialized vasculature (Table 2). These Col *bop1 bop2* phenotypes were observed at nearly the same ratio in *bop1 bop2* plants introgressed into L*er* (Table 2), indicating that *er* does not significantly contribute to the phenotypes. In *as1* and *as2* leaf petioles, partially abaxialized vein morphology was observed at a high frequency (Figures 7C, 7D, 7I, and 7J, Table 2). However, completely abaxialized vasculature consisting of xylem surrounded by phloem was not detected in *as1* and *as2* petioles (Table 2). The vascular patterning defects in the *bop1 bop2 as1* or *bop1 bop2 as2* leaf petioles were greatly enhanced compared with those of the parental plants (Figures 7E, 7F, 7K, and 7L, Table 2). These data indicate that *BOP1* and *BOP2* play redundant roles in adaxial-abaxial polarity specification in the leaf petiole and that their activity largely overlaps with that of *AS1* and *AS2*.

To better understand *BOP1* and *BOP2* function with respect to lateral organ polarity establishment, we examined the genetic interaction between *bop1 bop2* and *kan1 kan2* alleles. *KAN1* and *KAN2* function redundantly to promote abaxial organ identity,

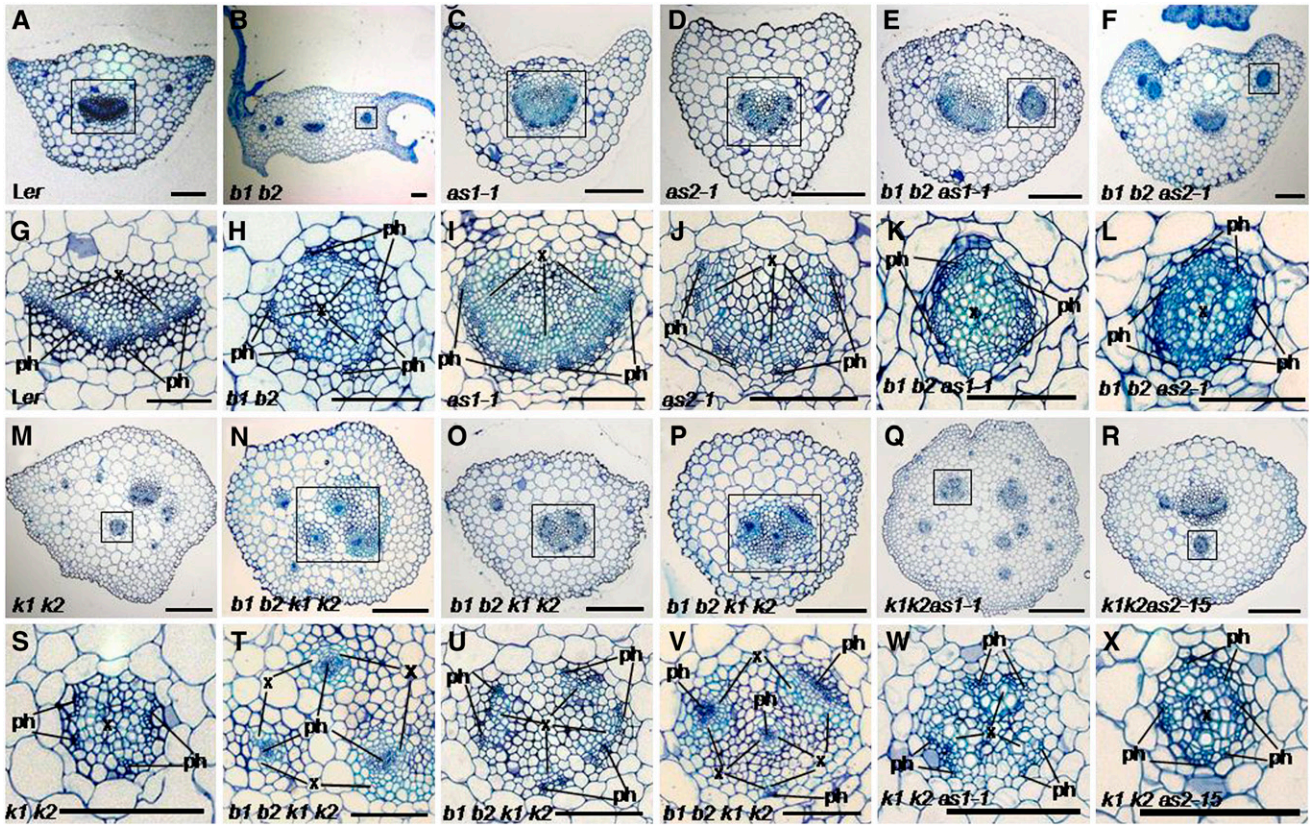

Figure 7. Histological Analysis of Leaf Petioles in Genetic Combinations between *bop1 bop2* and Organ Polarity Mutants.

Transverse sections were performed on rosette leaf petioles from wild-type (**[A]** and **[G]**), *bop1 bop2* (**[B]** and **[H]**), *as1-1* (**[C]** and **[I]**), *as2-1* (**[D]** and **[J]**), *bop1 bop2 as1-1* (**[E]** and **[K]**), *bop1 bop2 as2-1* (**[F]** and **[L]**), *kan1 kan2* (**[M]** and **[S]**), *kan1 kan2 as1-1* (**[Q]** and **[W]**), and *kan1 kan2 as2-1* plants (**[R]** and **[X]**). *bop1 bop2 kan1 kan2* radial leaf petiole (**[N]** to **[P]**) and (**[T]** to **[V]**). **(G)** to **(L)** and **(S)** to **(X)** are the magnified views of the regions boxed in **(A)** to **(F)** and **(M)** to **(R)**, respectively. ph, phloem; x, xylem; *b1 b2*, *bop1 bop2*; *k1 k2*, *kan1 kan2*. Bars = 200 μm in **(A)** to **(F)** and **(M)** to **(R)** and 100 μm in **(G)** to **(L)** and **(S)** to **(X)**.

and mutations in these genes cause adaxialized lateral organ development (Eshed et al., 2001, 2004). *kan1 kan2* plants had narrow leaves and developed ectopic outgrowths on their abaxial lamina (Figures 6M and 6Q; Eshed et al., 2001). *bop1 bop2 kan1 kan2* plants developed narrow leaves with ectopic blade outgrowth along the petioles, like *bop1 bop2* leaves, as well as ectopic outgrowths on their abaxial lamina, like *kan1 kan2* leaves (Figures 6N and 6R). However, all of the *bop1 bop2 kan1 kan2* leaves also showed extended, radialized petiole development that was not observed in either parental genotype (Figures 6N, 6O, and 6S, arrows). These data reveal a synergistic interaction between the *bop1 bop2* and *kan1 kan2* alleles in controlling lateral organ polarity in the basal regions of the leaf.

We better characterized the organ polarity phenotypes by analyzing the internal vascular patterning of the double and quadruple mutant leaves. The vasculature in more than half (55.9%) of *kan1 kan2* leaf petioles exhibited a pattern of phloem surrounded by xylem, representing an adaxialized phenotype (Table 2). This is consistent with the reported role of *KAN1* and *KAN2* in specifying abaxial organ identity (Eshed et al., 2001, 2004; Kerstetter et al., 2001). However, very surprisingly, 17.6% of *kan1 kan2* leaf petioles had abaxialized vasculature or a mixture of adaxialized and abaxialized vasculature (Figures 7M and 7S, Table 2). This observation suggests that *KAN1* and *KAN2* also contribute to the establishment of adaxial cell identity. We next examined the vascular patterning of *bop1 bop2 kan1 kan2* rosette leaf petioles and found that about nine-tenths of them exhibited abaxialized vasculature (Table 2). The exclusively adaxialized vasculature observed in *kan1 kan2* petioles was not detected in *bop1 bop2 kan1 kan2* petioles. The radialized portion of *bop1 bop2 kan1 kan2* leaves showed various kinds of organ polarity defects. The vascular bundles of nearly half of the leaves (44.0%) consisted of phloem surrounded by xylem (Figure 7T, Table 2), while one-third (36.0%) displayed xylem surrounded by phloem (Figures 7O and 7U, Table 2), and a small percentage (16.0%) had a mixture of both types of vasculature (Figures 7P and 7V, Table 2).

To know whether the vascular polarity defects occurred in other tissues, we examined the stem vasculature. The wild-type stem consists of multiple vascular bundles (see Supplemental Figure 4A online), each of which has xylem oriented toward the center in the adaxial position and phloem toward the periphery in

Table 2. Ratio of Vasculature Phenotypes in Rosette Leaf and Stem Organs

Lines	Total[a]	Ratio of Organ Vasculature Phenotypes (%)				
		Normal[b]	Abaxialized	Partially Abaxialized	Adaxialized	Mixed: Ab- and Adaxialized
Rosette Leaf Petiole						
L*er*	30	100	0	0	0	0
Col	29	100	0	0	0	0
bop1-4	31	100	0	0	0	0
bop2-11	31	100	0	0	0	0
bop1 bop2 (Col)[c]	27	22.2	22.2	55.6	0	0
bop1 bop2 (L*er*)[d]	21	19.0	23.8	57.1	0	0
as1-1	27	18.8	0	81.3	0	0
as2-1[e]	31	25.8	0	74.2	0	0
as2-15	18	33.3	0	66.7	0	0
bop1 bop2 as1-1	25	8.0	40.0	52.0	0	0
bop1 bop2 as2-1	30	0	93.3	6.7	0	0
bop1 bop2 as2-15	35	11.4	20.0	68.6	0	0
kan1 kan2	34	26.5	8.8	0	55.9	8.8
bop1 bop2 kan1 kan2[f]	32	6.3	87.5	0	0	6.3
bop1 bop2 kan1 kan2[g]	25	4.0	32.0	12.0	36.0	16.0
as1-1 kan1 kan2	21	19.0	61.9	9.5	0	9.5
as2-15 kan1 kan2	21	19.0	19.0	61.9	0	0
Stem						
L*er*	18	100	0	0	0	0
Col	22	100	0	0	0	0
bop1-4	21	100	0	0	0	0
bop2-11	22	100	0	0	0	0
bop1 bop2 (Col)[c]	18	100	0	0	0	0
bop1 bop2 (L*er*)[d]	17	100	0	0	0	0
as1-1	17	100	0	0	0	0
as2-1[e]	23	100	0	0	0	0
as2-15	21	100	0	0	0	0
bop1 bop2 as1-1	23	100	0	0	0	0
bop1 bop2 as2-1	22	100	0	0	0	0
bop1 bop2 as2-15	18	100	0	0	0	0
kan1 kan2	28	0	0	0	100	0
bop1 bop2 kan1 kan2	30	13.3	6.7	0	66.7	13.3
as1-1 kan1 kan2	20	40.0	0	0	60.0	0
as2-15 kan1 kan2	20	40.9	0	0	59.1	0

[a] Number of organs examined.
[b] Normal in stem means phloem in the peripheral outside region and xylem in the central inside region of the vasculature.
[c] *bop1 bop2* in the Col background.
[d] *bop1 bop2* backcrossed into L*er* one time.
[e] *as2-1* backcrossed into Col one time.
[f] Rosette leaf petioles were examined.
[g] Radialized leaf petioles were examined.

the abaxial position (see Supplemental Figure 4E online). The stem vasculature in *bop1 bop2* plants showed normal vein morphology (see Supplemental Figures 4B and 4F online), but all *kan1 kan2* stem vascular bundles displayed phloem surrounded by xylem, indicating adaxialized polarity (see Supplemental Figures 4C and 4G online; Table 2; Izhaki and Bowman, 2007). *bop1 bop2 kan1 kan2* stems had a decreased ratio of adaxialized vascular phenotypes compared with *kan1 kan2* stems (see Supplemental Figures 4D and 4H online; Table 2). Similar to what was observed in petioles, 6.7% of *bop1 bop2 kan1 kan2* stems exhibited an abaxialized phenotype of xylem surrounded by phloem, while others (13.3%) had both types of vasculature in a single stem (see Supplemental Figures 4I, 4J, 4M, and 4N online; Table 2).

Next, we analyzed genetic interactions between the *as1-1* or *as2-15* alleles and the *kan1 kan2* alleles. Approximately three-fourths of *as1 kan1 kan2* and *as2 kan1 kan2* leaf petiole vascular bundles were partially or fully abaxialized (71.4 and 80.9%, respectively; Figures 7Q, 7R, 7W, and 7X, Table 2). In addition, 9.5% of the *as1 kan1 kan2* leaf petioles displayed both adaxialized and abaxialized vascular bundles (Table 2). The stem vascular morphology of *as1* and *as2* plants is normal (data not

shown), whereas 40% of *as1 kan1 kan2* and *as2 kan1 kan2* stem veins exhibited xylem surrounded by phloem, which was not observed in the vasculature of *kan1 kan2* stems (see Supplemental Figures 4K, 4L, 4O, and 4P online; Table 2). Thus, the *as1* and *as2* mutations decreased the frequency of adaxialized vascular bundle formation in *kan1 kan2* leaves and stems. In contrast with the clear defects in internal tissue polarity observed in the double, triple, and quadruple mutants, we could not detect any significant polarity defects in epidermal cell morphogenesis using scanning electron microscopy (data not shown).

Regulation of Adaxial and Abaxial Polarity Genes by *BOP1* and *BOP2*

Our morphological and anatomical analyses implicate *BOP1* and *BOP2* in the specification of leaf polarity, suggesting that *BOP1* and *BOP2* might affect organ polarity gene expression. To investigate this idea, we used RT-PCR to examine the expression levels of several key organ polarity genes. *PHB* is one of the class III *HD-ZIP* genes that specify adaxial cell fate, and its steady state transcript levels were increased in 8-d-old *35S:BOP1* seedlings compared with wild-type seedlings (see Supplemental Figure 5 online). At this stage we could not detect a significant change in the expression levels of *FIL* and *KAN1*, which are restricted to abaxial leaf cells and promote their identity and/or growth. However, we found that *PHB* transcription was slightly upregulated, and *FIL* and *KAN1* transcription was slightly reduced in the developing young leaves of 22-d-old *35S:BOP1* leaves compared with wild-type leaves (see Supplemental Figure 5 online). Neither gene showed detectable changes in its mRNA transcript levels in *bop1-4*, *bop2-11*, or *bop1-4 bop2-11* plants (data not shown). These results show that *PHB*, *FIL*, and *KAN1* transcript levels are misregulated in *35S:BOP1* leaves, although not sufficiently to cause a detectable polarity phenotype in these organs.

Although the transcript levels of the organ polarity genes appeared unaltered in *bop* mutant plants, it remained possible that the spatial expression patterns of these genes were perturbed. Thus, we examined the expression patterns of the polarity genes using RNA in situ hybridization. In wild-type plants, *FIL* expression is restricted to the abaxial side of the developing leaf (Figure 8A; Sawa et al., 1999; Siegfried et al., 1999). In *as2*, *as1*, and *kan1 kan2* leaves, *FIL* transcripts are detected in the correct abaxial domain (Figures 8B to 8D). Similarly, in *bop1 bop2*, *bop1 bop2 as2*, *bop1 bop2 as1*, and *bop1 bop2 kan1 kan2* plants, *FIL* expression was detected on the abaxial side of initiating and young leaf primordia (Figures 8K to 8N). However, more mature *bop1 bop2*, *bop1 bop2 as2*, *bop1 bop2 as1*, and *bop1 bop2 kan1 kan2* leaves exhibited ectopic *FIL* transcription in the adaxial domain (Figures 8K to 8N, arrows). The differentiated leaves of *bop1 bop2* plants exhibited *FIL* expression on the adaxial side of the primordial ectopic organ outgrowths (Figure 8P, arrows), while *FIL* transcripts were not detected in differentiated leaves of Col plants (Figure 8F). *FIL* transcripts were likewise detected on the adaxial side of *bop1 bop2 as2*, *bop1 bop2 as1*, and *bop1 bop2 kan1 kan2* differentiated leaves but with the expression in the more central region of the leaf (Figures 8Q to 8S, arrows). By contrast, no *FIL* expression was detected in *as2*, *as1*, or *kan1 kan2* differentiated leaves (Figures 8G to 8I). Like *FIL* transcripts, *KAN1* transcripts are restricted to the abaxial domain of wild-type leaves (Figure 8O). However, in *bop1 bop2* leaves, *KAN1* expression is detected in the adaxial region in the area in which the ectopic organ outgrowths develop (Figure 8T). Taken together, these data demonstrate that *BOP1* and *BOP2* play a role in regulating the spatial expression domains of the abaxial polarity regulatory genes *FIL* and *KAN1*.

In wild-type seedlings, *PHV* expression becomes restricted to the vasculature and the adaxial region of initiating rosette leaf primordia (Figure 9A; Eshed et al., 2001; McConnell et al., 2001; Emery et al., 2003). The domain of *PHV* expression is unaltered in *as2* and *as1* seedlings (Figures 9B and 9C). In *kan1 kan2* seedlings, *PHV* expression is detected throughout the leaf primordia, but a stronger signal is observed on the adaxial side than on the abaxial side (Figure 9D), suggesting that these organs still maintain some residual asymmetry. Developing young leaves of *bop1 bop2*, *bop1 bop2 as2*, *bop1 bop2 as1*, and *bop1 bop2 kan1 kan2* seedlings exhibited *PHV* expression in the normal adaxial domain (Figures 9I to 9L). However, in *bop1 bop2 kan1 kan2* leaves, *PHV* expression is restricted to a smaller area of the adaxial domain than in *kan1 kan2* leaves (Figures 9D and 9L, arrow). This result indicates that, whereas the young leaves of *kan1 kan2* plants have adaxialized organ identity, the young leaves of quadruple mutant plants acquire abaxialized organ identity, which is consistent with histological data. *PHV* expression is not detected in the differentiated leaves of Col, *as2*, *as1*, and *kan1 kan2* plants (Figures 9E to 9H) but can be observed on the adaxial side of the differentiated leaves of *bop1 bop2*, *bop1 bop2 as2*, *bop1 bop2 as1*, and *bop1 bop2 kan1 kan2* plants (Figures 9I to 9P, arrows). Furthermore, *PHV* was expressed more centrally in *bop1 bop2 as2*, *bop1 bop2 as1*, and *bop1 bop2 kan1 kan2* leaves than in *bop1 bop2* leaves (Figures 9M to 9P, arrows). In summary, in situ hybridization data from *bop1 bop2*, *bop1 bop2 as2*, *bop1 bop2 as1*, and *bop1 bop2 kan1 kan2* rosette leaves indicate that *BOP1* and *BOP2* act to specify adaxial organ identity.

DISCUSSION

Functional Relationship between *BOP1* and *BOP2*

Our data show that *BOP1* and *BOP2* have unique and shared functions in *Arabidopsis* development. *bop1* and *bop2* single mutants display phenotypes in distinct tissues, with *bop1* plants exhibiting defects in rosette leaf development and *bop2* plants showing phenotypes exclusively in inflorescence and flower development (see Supplemental Figure 2 and Supplemental Table 1 online). This suggests that although both *BOP1* and *BOP2* have high sequence homology and almost identical expression patterns (Ha et al., 2004; Hepworth et al., 2005; Norberg et al., 2005), the requirement for the two genes differs in different tissues, with *BOP1* being more important for leaf development and *BOP2* more important for flower development.

The *bop1-1* allele was formally characterized as having a dominant-negative genetic character (Ha et al., 2004). A straightforward explanation for the behavior of this allele is that the mutant bop1-1 protein interferes with the activity of the related BOP2 protein, which can otherwise largely compensate for the

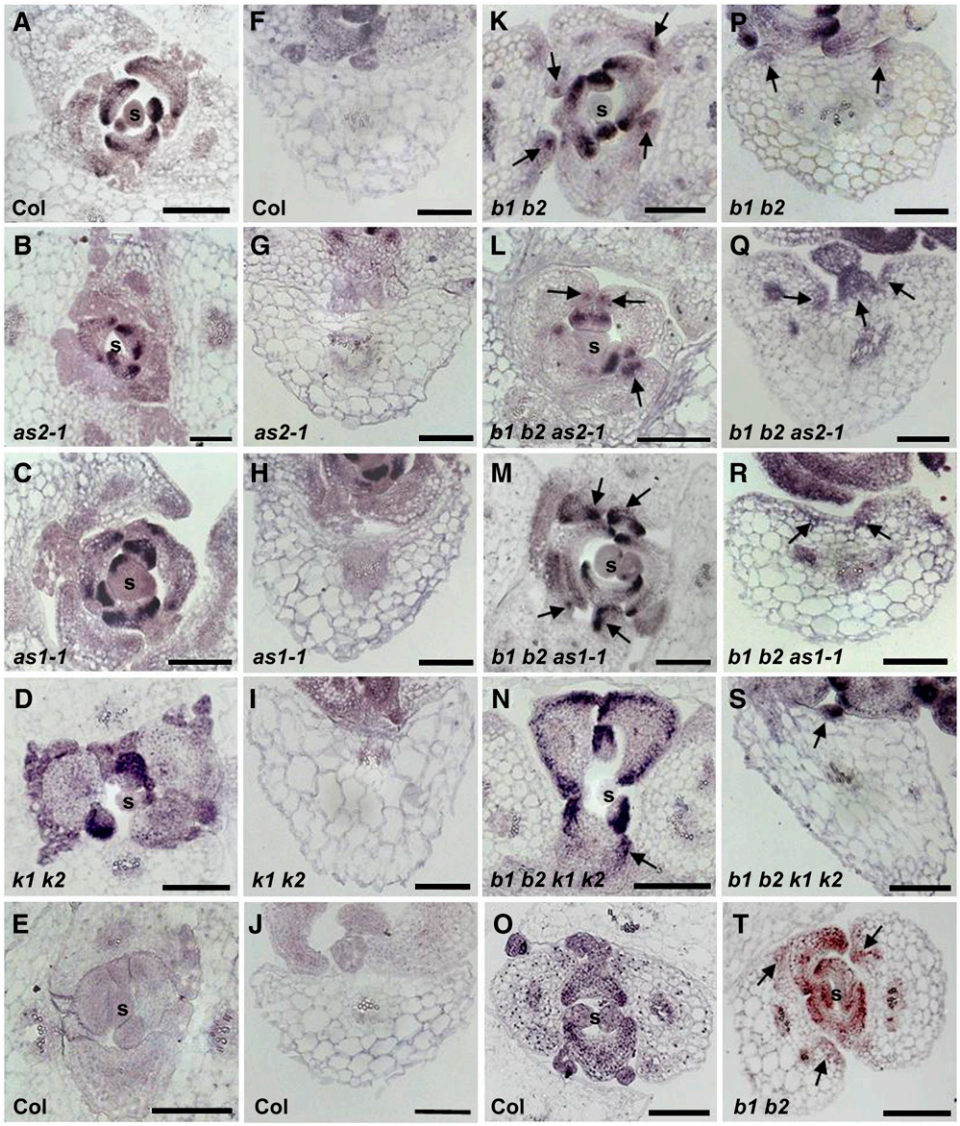

Figure 8. RNA in Situ Hybridization Analysis of *FIL* and *KAN* Expression.

(A) to **(N)** and **(P)** to **(S)** RNA in situ hybridization analysis of *FIL* expression in 9-d-old Col (**[A]**, **[E]**, **[F]**, and [**J**]), *as2-1* (**[B]** and **[G]**), *as1-1* (**[C]** and **[H]**), *kan1 kan2* (**[D]** and **[I]**), *bop1 bop2* (**[K]** and **[P]**), *bop1 bop2 as2-1* (**[L]** and **[Q]**), *bop1 bop2 as1-1* (**[M]** and **[R]**), and *bop1 bop2 kan1 kan2* (**[N]** and **[S]**). **(E)** and **(J)** show the sense control.

(O) and **(T)** RNA in situ hybridization analysis of *KAN* expression in 9-d-old Col **(O)** and *bop1 bop2* plants **(T)**. Arrows indicate *FIL* or *KAN* ectopic expression.

s, shoot meristem region; *b1 b2*, *bop1 bop2*; *k1 k2*, *kan1 kan2*. Bars = 100 μm.

lack of BOP1 activity during lateral organ formation. However, *bop1-1* plants have much weaker inflorescence and flower phenotypes than *bop1 bop2* plants (Ha et al., 2003; Hepworth et al., 2005; Norberg et al., 2005), suggesting that bop1-1 protein might not completely abolish BOP2 function in these tissues.

Role of *BOP1* and *BOP2* in Lateral Organ Formation

The formation of a lateral organ from the flanks of the SAM requires the repression of the class I *knox* genes by *AS1* and *AS2* (Byrne et al., 2000, 2002) and the establishment of a boundary between the meristem and the primordium that demarcates their separate fates. *AS1* and *AS2*, along with *BP*, have been shown to positively regulate *LOB* expression along this boundary (Byrne et al., 2002). Based on genetic interactions, *AS1* and *AS2* are proposed to act in a common hierarchy that promotes lateral organ cell fate by repressing *BP* and *KNAT2* and inducing *LOB* (Byrne et al., 2002). Here, we have demonstrated a key role for *BOP1* and *BOP2* in this cell fate regulatory hierarchy.

Expression of the class I *knox* genes *BP*, *KNAT2*, and *KNAT6* is increased in *bop1-1* (Ha et al., 2003) and *bop1-4 bop2-11* plants (Figure 2A), implicating *BOP1* and *BOP2* in the negative regulation

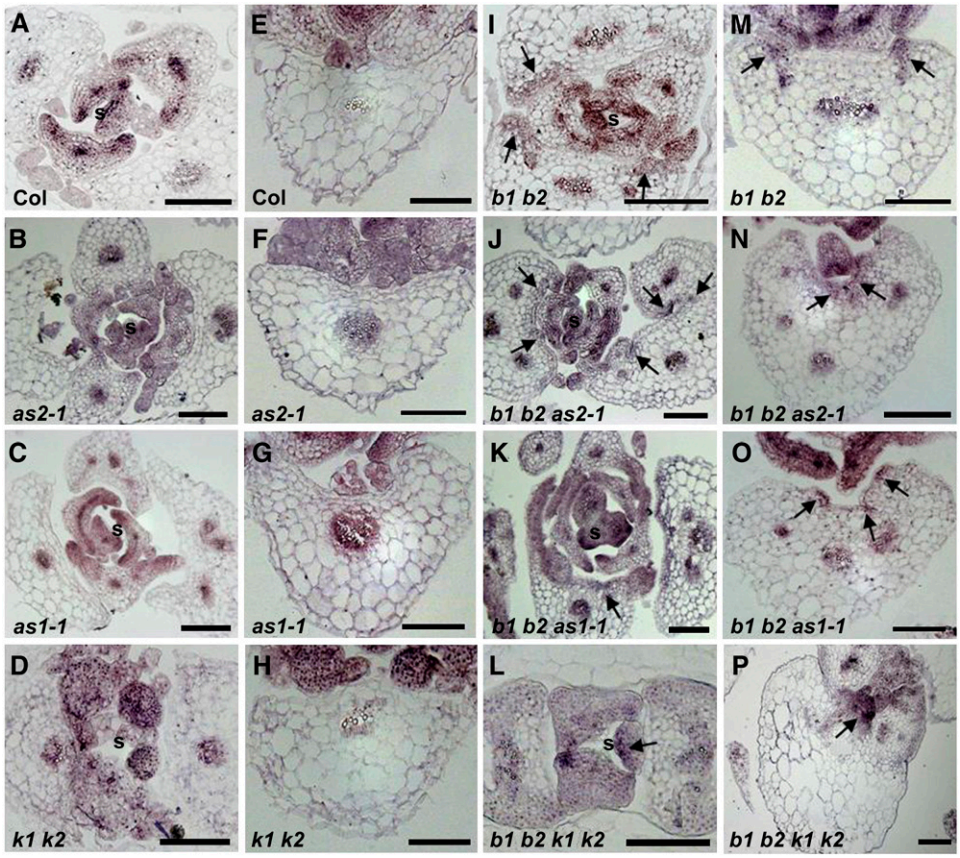

Figure 9. RNA in Situ Hybridization Analysis of *PHV* Expression.

RNA in situ hybridization analysis of *PHV* expression in 9-d-old Col (**[A]** and **[E]**), *as2-1* (**[B]** and **[F]**), *as1-1* (**[C]** and **[G]**), *kan1 kan2* (**[D]** and **[H]**), *bop1 bop2* (**[I]** and **[M]**), *bop1 bop2 as2-1* (**[J]** and **[N]**), *bop1 bop2 as1-1* (**[K]** and **[O]**), and *bop1 bop2 kan1 kan2* (**[L]** and **[P]**). Arrows indicate ectopic expression of *PHV*. s, shoot meristem region; *b1 b2*, *bop1 bop2*; *k1 k2*, *kan1 kan2*. Bars = 100 μm.

of *knox* gene activity. *35S:BOP1* and *35S:BOP2* plants show a corresponding decrease in *BP* transcript levels (Figures 2B and 2C), indicating that *BP* responds quantitatively to *BOP1* and *BOP2*. Expression of both *BOP1* and *BOP2* is detected at the base of flowers, including the pedicel (Ha et al., 2003; Hepworth et al., 2005; Norberg et al., 2005), and *BOP1:GUS* is expressed in nodes and stems (C.M. Ha and J.C. Fletcher, unpublished data). These expression domains overlap with those of *BP* (Douglas et al., 2002; Venglat et al., 2002), consistent with *BOP1* potentially repressing *BP* in nodes and stems as well as leaf primordia. *bp* plants form shortened internodes and downward-orienting siliques, indicating a role for *BP* in stem and pedicel differentiation (Douglas et al., 2002; Venglat et al., 2002). The downward-orienting silique phenotype of *35S:BOP1* and *35S:BOP2* plants may therefore result from strong suppression of *BP* transcription by highly expressed *BOP1* or *BOP2*.

We identified three *LOB* domain genes as targets of positive regulation by *BOP1* and *BOP2*: *AS2*, *LOB*, and *LBD36/ASL1*. *AS2* expression levels are reduced in *bop* mutant plants and elevated in *35S:BOP1* and *35S:BOP2* plants (Figures 3A and 3B), indicating that *BOP1* and *BOP2* are required for *AS2* induction. However, *AS2* activation does not depend entirely on the action of *BOP1* and *BOP2*, since a small amount of *AS2* transcript is present in *bop1-4 bop2-11* plants (Figure 3B). However, we could not rule out the possibility that the BTB/POZ domain regions of *BOP1* and *BOP2* might be transcribed in *bop1-4 bop2-11* plants, which could activate *AS2*. To test this possibility, we examined *AS2* expression in *bop1-7 bop2-12* plants that contain T-DNA insertions in the BTB/POZ domains of *BOP1* and *BOP2*. These plants lack either partial- or full-length transcripts of *BOP1* and *BOP2* and show the same morphological defects as *bop1-4 bop2-11* plants. We could still detect *AS2* transcripts at a low level in *bop1-7 bop2-12* plants (C.M. Ha and J.C. Fletcher, unpublished data), indicating that a BOP-independent pathway also contributes to *AS2* activation. *BOP1* and *BOP2* expression is unchanged in *as2* mutants, revealing that *AS2* is downstream of *BOP1* and *BOP2* at the level of transcriptional regulation.

Does *AS2* mediate all the functions of *BOP1* and *BOP2* in leaf development? Like *BOP1* and *BOP2*, *AS2* negatively regulates class I *knox* gene expression in leaves (Byrne et al., 2000; Ori et al., 2000; Semiarti et al., 2001; Sun et al., 2002). Ectopic expression of *AS2* causes a similar, though not identical, effect to that of ectopic *BOP1* and *BOP2* (Lin et al., 2003; Xu et al., 2003), and some *35S:BOP1* phenotypes are attenuated in an *as2-101*

background. It is therefore possible that reduced *AS2* function causes the *bop1-1* and *bop1 bop2* leaf phenotypes. However, *bop1-1 as2-1* and *bop1 bop2 as2-1* plants have synergistic phenotypes (Ha et al., 2003; this study), rather than the epistatic phenotypes that would be expected if loss of *AS2* expression were the sole cause of the *bop* leaf phenotypes. Further, the *35S:AS2* construct does not rescue the *bop1-1* leaf phenotypes. Thus, although *AS2* acts downstream of *BOP1* and *BOP2*, the regulation of leaf development by *BOP1* and *BOP2* is not exclusively mediated through *AS2*.

Another target of positive regulation by the *BOP1* and *BOP2* genes is *LOB*, which is thought to play a role in establishing a boundary between the SAM and initiating lateral organs (Shuai et al., 2002). *BOP1* and *BOP2* act redundantly to promote *LOB* expression at the meristem-leaf boundary (Figures 3A and 3B), and *BOP1* is sufficient to induce *LOB* transcription in certain developmental contexts (Figure 4). *LOB* is activated by *AS1* and *AS2*, so the simplest scenario would be that *BOP1* and *BOP2* activate *AS2* expression, and then *AS2* activates *LOB* expression. However, *BOP1* overexpression but not *AS2* overexpression is sufficient to induce ectopic *LOB* activation (Figure 3A), suggesting either that *BOP1* can induce *LOB* through an *AS2*-independent mechanism or that *BOP1* functions together with *AS2* to activate *LOB* specifically at the meristem-organ boundary. Interestingly, although *35S:LOB* plants are small and exhibit hyponastic leaf morphology (Shuai et al., 2002) similar to that of *35S:BOP1* and *35S:BOP2* plants, *LOB* does not condition the *BOP* overexpression phenotypes. Potentially other *LBD* family genes, such as *LBD36*/*ASL1*, may contribute along with *AS2* to generating the *35S:BOP* phenotypes.

The expression pattern of *LBD36*/*ASL1* is broad and overlaps with that of *BOP1* and *BOP2* (Chalfun-Junior et al., 2005), and like *LOB*, its transcription responds positively as *BOP1* and *BOP2* expression increases (Figure 3A). Dominant, activation-tagged *isoginchaku-3D* (*iso-3D*), *iso-4D*, and *downwards siliques-1D* plants that overexpress *LBD36*/*ASL1* display *bp*-like phenotypes and have reduced *BP* mRNA levels (Nakazawa et al., 2003; Chalfun-Junior et al., 2005), suggesting that the repression of *BP* transcription in *35S:BOP1* and *35S:BOP2* plants might be mediated, at least in part, via their induction of *LBD36*/*ASL1*. It remains to be seen whether additional genes in the 42-member *LBD* family are also regulated by *BOP1* and *BOP2*.

BOP1 and *BOP2* Act Redundantly with *AS1* and *AS2* to Regulate Lateral Organ Polarity

Our study has shown that *bop1 bop2* double mutants have abaxialized leaf petiole vasculature (Figure 7H, Table 2). This lateral organ polarity defect was strongly enhanced by mutations in either *as1* or *as2* (Figures 7K and 7L, Table 2), demonstrating that *BOP1* and *BOP2* function redundantly with the *AS1-AS2* pathway to regulate adaxial organ identity. A question that then arises is why ectopic expression of *BOP1* or *BOP2* does not cause widespread adaxialization of structures such as stem vasculature and leaf mesophyll and vascular tissue. A trivial possibility is that the level of ectopic *BOP1* or *BOP2* transcription in the 35S lines is not sufficient to trigger a detectable polarity shift. Alternatively, BOP1/2 activity may require the presence of localized cofactors that are not themselves misexpressed in the 35S lines, thus leading to a limited set of overexpression phenotypes.

Our data suggest that *BOP1* and *BOP2* promote adaxial cell fate together with *AS1* or *AS2* during cellular differentiation in the leaf petiole, after the initial establishment of the adaxial-abaxial polarity axis via interaction between class III HD-ZIP and *KAN* family genes. In *bop1 bop2 as2* and *bop1 bop2 as1* plants, radialized organs develop extensively along the petioles of more mature rosette leaves (Figures 6D and 6F). Furthermore, the initiating leaf primordia of *bop1 bop2*, *bop1 bop2 as2*, *bop1 bop2 as1*, and *bop1 bop2 kan1 kan2* plants display normal *FIL* and *PHV* expression patterns, yet ectopic *FIL* and reduced *PHV* expression is detected in more mature rosette leaves in which petiole differentiation is clearly visible (Figures 8L and 8M). These results indicate that *BOP1* and *BOP2* play an important role in maintaining adaxial cell fate at this later stage. The lack of alteration in the *FIL* and *PHV* expression patterns in initiating leaf primordia of *bop1 bop2* plants may be explained by redundant functions of other genes, such as *AE3* (Huang et al., 2006), resulting in nearly normal blade morphogenesis in *bop1 bop2* plants.

A longstanding model holds that the juxtaposition of adaxial and abaxial cellular domains is required for outgrowth of the leaf blade, or lamina (Waites and Hudson, 1995). This outgrowth seems to be mediated, at least in part, though *YAB* gene activity (Eshed et al., 2004). Mutations in *BOP1* and *BOP2* activate and expand the transcription of the *YAB* gene *FIL* into the adaxial marginal regions of the leaf, demonstrating that *BOP1* and *BOP2* are required to repress *FIL* expression in this domain. Ectopically expressed *FIL*, juxtaposed with ectopically expressed *PHV* on the upper side of *bop1 bop2*, *bop1 bop2 as2*, *bop1 bop2 as1*, and *bop1 bop2 kan1 kan2* petioles (Figures 8 and 9), may be sufficient to generate new boundaries of adaxial and abaxial gene expression. In wild-type plants, the margins of the petiole display a small and undifferentiated cellular character, indicating the maintenance of proliferative activity in these regions. Thus, in *bop1 bop2* plants, the combination of a less differentiated cellular state with the juxtaposition of adaxial and abaxial gene expression in the petiole margin would result in the development of a new boundary region sufficient for ectopic organ outgrowth in that region. Taken together, these data suggest that *BOP1*, *BOP2*, *AS1*, and *AS2* act redundantly to repress abaxial organ identity gene expression in the rosette leaf petiole and, as a result, promote adaxial organ identity. This in turn maintains the cellular fate of the leaf petiole in a differentiated state.

Our data reveal that *BOP1* and *BOP2* can also contribute to patterning the stem vasculature because mutations in both *BOP1* and *BOP2* partially reversed the *kan1 kan2* adaxialized stem vasculature phenotypes (see Supplemental Figure 4 online; Table 2). Mutations in *AS1* or *AS2* likewise decreased the frequency of adaxialized vasculature formation in *kan1 kan2* stems. Currently, we have no evidence that either *BOP1* or *BOP2* is expressed in the provascular tissue of the shoot meristem, suggesting that a downstream component(s) of the regulatory pathway may act non-cell-autonomously to control adaxial-abaxial polarity during stem vascular patterning.

KAN1 and *KAN2* Promote Both Abaxial and Adaxial Organ Identity

Loss of *KAN* activity results in leaf adaxialization, implicating the *KAN* genes in specification of abaxial cell identity (Eshed et al., 2001, 2004; Kerstetter et al., 2001; Emery et al., 2003). In this study, we have shown that some *kan1 kan2* rosette leaf petioles develop abaxialized vasculature (Figure 7S). Furthermore, this novel role for *KAN1* and *KAN2* is strongly enhanced in the *bop1 bop2*, *as1*, and *as2* mutant backgrounds (Figures 7T to 7X, Table 2). Thus, *KAN1* and *KAN2* may function to promote adaxial organ identity redundantly with *BOP1*, *BOP2*, *AS1*, and *AS2* in addition to their well-known role in establishing abaxial organ identity.

A dual function in adaxial-abaxial polarity regulation has also been observed for the *YAB* gene *GRAMINIFOLIA* (*GRAM*), the *Antirrhinum* ortholog of *FIL* (Golz et al., 2004; Navarro et al., 2004). Like *FIL*, *GRAM* is expressed abaxially in developing *Antirrhinum* organs and is required for abaxial cell identity and growth at the leaf margins. Interestingly, the *gram* mutation also causes adaxial mesophyll cells away from the leaf margin to partially resemble abaxial spongy mesophyll cells, and *gram* plants occasionally develop needle-like leaves in which xylem is surrounded by phloem. Thus, *GRAM* is also needed to establish adaxial organ identity in some regions of the *Antirrhinum* leaf. In contrast with *gram* mutants, *Arabidopsis fil yab3* mutants only show adaxialized lateral organ development (Siegfried et al., 1999). It will thus be interesting to examine whether *FIL* and *YAB3* have lost *GRAM*-like functions or if *GRAM* acquired new functions during evolution.

METHODS

Plant Materials and Genetics

The *bop1-4* allele in the Col ecotype was described previously (Ha et al., 2004). The *bop2-11* (N55227) allele was obtained from the Nottingham Arabidopsis Stock Centre and is in the Col ecotype. *as1-1* Col (CS3374), *as2-1* ER (CS3117), *bp-1* (CS30), and Lan (CS1304) seeds were obtained from the ABRC. *as1-101* and *as2-101* seeds in the L*er* ecotype were kindly provided by Hai Huang (Chinese Academy of Sciences, China), *as2-15* seeds in the Col ecotype by Gerco Angenent (Plant Research International, The Netherlands), and *kan1-2 kan2-1* seeds in the L*er* ecotype by John Bowman (University of California, Davis). The *lob:ET22* enhancer-trap line was a gift from Patty Springer (University of California, Riverside). *Arabidopsis thaliana* plants were grown as described previously (Ha et al., 2004).

To generate *bop1 bop2 as1* or *bop1 bop2 as2* plants, *bop1 bop2* plants were crossed with *as1* or *as2* plants. *bop1 bop2 kan1 kan2*, *as1 kan1 kan2*, or *as2 kan1 kan2* plants were isolated from crosses between *bop1 bop2*, *as1*, or *as2* and *kan1 kan2*/+ plants. Plants with novel phenotypes in the F2 generation of the *kan1 kan2*/+ crosses were selected and genotyped using the primers KAN1-F (5′-TGAGCTCAAGAACCGACTT-3′) and KAN2-F (5′-TTAGCTGGGAATCTTGGCA-3′). When crosses were performed between mutants in different ecotypes, such as *bop1-4 bop2-11* in Col to *as2-1* in the ER background, control crosses were performed of the relevant mutant into Col to control for background genetic variation.

Construction of Transgenic Plants

Constructs for *BOP* overexpression were generated by amplifying the *BOP1* and *BOP2* coding regions from L*er* seedling cDNA using the primers BOP1-F (5′-AGATCTAA-ATCAACAAAGGAGCTATGAGC-3′) and BOP1-R (5′-GGTCACCGATGATAGGG-ACTACAAAAAGAC-3′) or BOP2-F (5′-CCATGGAGATGAGCAATCTTGAAGAA-3′) and BOP2-R (5′-GGTCCACCGAGAACTAGAAGTGATGTTG-3′). Each PCR product was sequenced and placed downstream of the 35S promoter in the pCAMBIA1302 binary vector (CAMBIA). The *35S:AS2* construct was kindly provided by Patty Springer (University of California, Riverside). For each construct, the binary vector in the *Agrobacterium tumefaciens* strain GV3101 was introduced into L*er* plants by the floral dip method (Clough and Bent, 1998). Transformants were selected on Murashige and Skoog medium containing 50 μM hygromycin.

Expression Analysis

For RT-PCR studies, cDNA was synthesized from 5 μg of total RNA using an oligo(dT_{15}) primer and SuperScript III reverse transcriptase (Invitrogen). One microliter of the first-strand cDNA reaction was used as a template for PCR amplification. PCR conditions for *BOP1* and *BOP2* amplification were as follows: denaturation at 94°C for 3 min, followed by 27 to 33 cycles of 94°C for 35 s, 55°C for 45 s, and 72°C for 1 min, using primers BOP1-RT-76R (5′-GTGAATCTGATCCTTCGCAACC-3′), BOP1-24-76F (5′-ATCCAAACTACTTCC-GCTCGTG-3′), BOP2-RT-2R (5′-TAT-AGACCCGACCCAACATGG G-3′), and BOP2-RT-2F (5′-TCATTCATAT-GAGGGTAAATCCCG-3′). PCR conditions for *BP*, *KNAT2*, and *KNAT6* amplification were as follows: denaturation at 94°C for 3 min, followed by 33 cycles of 94°C for 35 s, 53°C for 50 s, and 72°C for 1 min, using primers KNAT1-F (5′-GATGATCCCATATTGTCACTCTTCCC-3′), KNAT1-R (5′-ATGGAAGAATACCAGCAT-GACAAC-3′), KNAT2-F (5′-CCGAAGG-CTTCCAATGGCG-3′), KNAT2-R (5′-GCGGCGATCACTGATCGTATC-3′), KNAT6-F (5′-TCATTCCTCGGTAAAGAATGATCCACTAG-3′), and KNAT6-R (5′-ATCTACAATTTCCATTCGGCCGGTG-3′) (Semiarti et al., 2001). PCR conditions for *AS1*, *AS2*, and *LOB* amplification were as follows: denaturation at 94°C for 3 min, followed by 28 to 38 cycles of 94°C for 35 s, 54°C for 45 s, and 72°C for 1 min. Gene-specific primers for *LOB* and *AS1* were as previously published (Shuai et al., 2002; Lin et al., 2003).

For amplification of *PHB*, *FIL*, and *KAN1* cDNAs, the following gene-specific primers were used: PHB-5 (5′-TGATGGTCCATTCGATGAGC-3′), PHB-3 (5′-TCTAAACTCACGAGGCCGCA-3′), FIL-3 (5′-GCTATGTCCA-ATGCAACTTT-3′), FIL-4 (5′-TTCTTGGCAGCAGCACTAAA-3′), KAN1-5 (5′-ACAACAACGCTTACCGATCA-3′), and KAN1-R (5′-ATTTCTCGTGC-CAATCTGGT-3′) (Lin et al., 2003). PCR conditions for these genes were as follows: denaturation at 94°C for 3 min, followed by 33 cycles of 94°C for 35 s, 56°C for 45 s, and 72°C for 1 min. *LBD36/ASL1* cDNA was amplified using the same PCR conditions used for *LOB* cDNA amplification, with the primers LBD36-F2 (5′-TAATTGAGGCTCTCAAGTCT-3′) and LBD36-R2 (5′-ACCAATGACATTCCTTCTAC-3′). *Arabidopsis TUB4* was used as an internal control (Ha et al., 2003). Quantification of RT-PCR was performed using the Scion Image program.

Histology and Microscopy

lob bop1-1 and *lob bop1-4 bop2-11* homozygous plants and *lob 35S:BOP1* and *lob 35S:BOP2* T1 plants were selected and stained for GUS activity as described previously (Jun et al., 2002). Samples for histological analysis were fixed and prepared as described previously (Ha et al., 2003). Plant tissue sections (3 to 4 μm thick) were cut with a rotary microtome (MICROM International) and stained with methylene blue.

In Situ Hybridization

Plant fixation and in situ hybridization were performed as described previously (Jackson, 1992). For the *BOP1* and *KAN1* probes, the full-length cDNA sequences were amplified and cloned in the pBluescript KS+ plasmid (Stratagene). *PHV* and *FIL* probes were generated as

previously described (Eshed et al., 2001). Probes for in situ hybridization were transcribed using the digoxigenin labeling mix (Roche).

Supplemental Data

The following materials are available in the online version of this article.

Supplemental Figure 1. *BOP1* and *BOP2* Expression in Wild-Type and *bop* Mutant Plants.

Supplemental Figure 2. Phenotypes of *bop* Mutant Plants.

Supplemental Figure 3. Histological Analysis of Vegetative Shoot Apices.

Supplemental Figure 4. Histological Analysis of Stem Vasculature in Genetic Combinations between *bop1 bop2* and Organ Polarity Mutants.

Supplemental Figure 5. Expression of Polarity Genes in *BOP1* Overexpressor Plants.

Supplemental Table 1. Phenotypes of *bop* Mutant Plants.

ACKNOWLEDGMENTS

We thank Patty Springer for the *lob:ET22* seeds and *35S:AS2* construct, Hai Huang for the *as1-101* and *as2-101* seeds, Gerco Angenent for the *as2-15* seeds, and John Bowman for the *kan1-2 kan2-1* seeds. We also thank the ABRC for supplying mutant seeds and the Nottingham Arabidopsis Stock Centre for providing insertion lines. We thank Cristel Carles and Ludmila Tyler for critical reading of the manuscript. This work was supported by a USDA Current Research Information System grant to J.C.F. H.G.N. was supported by the National Core Research Center for Systems Biodynamics and the Crop Functional Genomics Center, Korea.

Received March 30, 2007; revised May 29, 2007; accepted June 7, 2007; published June 29, 2007.

REFERENCES

Adenot, X., Elmayan, T., Lauressergues, D., Boutet, S., Bouche, N., Gasciolli, V., and Vaucheret, H. (2006). DRB4-dependent TAS3 trans-acting siRNAs control leaf morphology through AGO7. Curr. Biol. **16:** 927–932.

Bao, N., Lye, K.W., and Barton, M.K. (2004). MicroRNA binding sites in Arabidopsis class III HD-ZIP mRNAs are required for methylation of the template chromosome. Dev. Cell **7:** 653–662.

Byrne, M.E., Barley, R., Curtis, M., Arroyo, J.M., Dunham, M., Hudson, A., and Martienssen, R.A. (2000). *Asymmetric leaves1* mediates leaf patterning and stem cell function in *Arabidopsis*. Nature **408:** 967–971.

Byrne, M.E., Simorowski, J., and Martienssen, R.A. (2002). *ASYMMETRIC LEAVES1* reveals *knox* gene redundancy in *Arabidopsis*. Development **129:** 1957–1965.

Chalfun-Junior, A., Franken, J., Mes, J.J., Marsch-Martinez, N., Pereira, A., and Angenent, G. (2005). *ASYMMETRIC LEAVES2-LIKE1* gene, a member of the AS2/LOB family, controls proximal-distal patterning in *Arabidopsis* petals. Plant Mol. Biol. **57:** 559–575.

Clough, S.J., and Bent, A.F. (1998). Floral dip: A simplified method for Agrobacterium-mediated transformation of *Arabidopsis thaliana*. Plant J. **16:** 735–743.

Douglas, S.J., Chuck, G., Dengler, R.E., Pelecanda, L., and Riggs, C.D. (2002). *KNAT1* and *ERECTA* regulate inflorescence architecture in Arabidopsis. Plant Cell **14:** 547–558.

Emery, J.F., Floyd, S.K., Alvarez, J., Eshed, Y., Hawker, N.P., Izhaki, A., Baum, S.F., and Bowman, J.L. (2003). Radial patterning of *Arabidopsis* shoots by class III HD-ZIP and *KANADI* genes. Curr. Biol. **13:** 1768–1774.

Eshed, Y., Baum, S.F., and Bowman, J.L. (1999). Distinct mechanisms promote polarity establishment in carpels of Arabidopsis. Cell **99:** 199–209.

Eshed, Y., Baum, S.F., Perea, J.V., and Bowman, J.L. (2001). Establishment of polarity in lateral organs of plants. Curr. Biol. **11:** 1251–1260.

Eshed, Y., and Bowman, J.L. (2004). MicroRNAs guide asymmetric DNA modifications guiding asymmetric organs. Dev. Cell **7:** 629–630.

Eshed, Y., Izhaki, A., Baum, S.F., Floyd, S.K., and Bowman, J.L. (2004). Asymmetric leaf development and blade expansion in *Arabidopsis* are mediated by KANADI and YABBY activities. Development **131:** 2997–3006.

Fahlgren, N., Montgomery, T.A., Howell, M.D., Allen, E., Dvorak, S.K., Alexander, A.L., and Carrington, J.C. (2006). Regulation of AUXIN RESPONSE FACTOR3 by TAS3 ta-siRNA affects developmental timing and patterning in Arabidopsis. Curr. Biol. **16:** 939–944.

Garcia, D., Collier, S.A., Byrne, M.E., and Martienssen, R.A. (2006). Specification of leaf polarity in Arabidopsis via the trans-acting siRNA pathway. Curr. Biol. **16:** 933–938.

Golz, J.F., Roccaro, M., Kuzoff, R., and Hudson, A. (2004). *GRAMINIFOLIA* promotes growth and polarity of *Antirrhinum* leaves. Development **131:** 3661–3670.

Ha, C.M., Jun, J.H., Nam, H.G., and Fletcher, J.C. (2004). *BLADE-ON-PETIOLE1* encodes a BTB/POZ domain protein required for leaf morphogenesis in Arabidopsis thaliana. Plant Cell Physiol. **45:** 1361–1370.

Ha, C.M., Kim, G.-T., Kim, B.C., Jun, J.H., Soh, M.S., Ueno, Y., Machida, Y., Tsukaya, H., and Nam, H.G. (2003). The *BLADE-ON-PETIOLE1* gene controls leaf pattern formation through the modulation of meristematic activity in Arabidopsis. Development **130:** 161–172.

Hepworth, S.R., Zhang, Y., McKim, S., Li, X., and Haughn, G. (2005). BLADE-ON-PETIOLE-dependent signaling controls leaf and floral patterning in Arabidopsis. Development **17:** 1434–1448.

Huang, W., Pi, L., Liang, W., Xu, B., Wang, H., Cai, R., and Huang, H. (2006). The proteolytic function of the *Arabidopsis* 26S proteasome is required for specifying leaf adaxial identity. Plant Cell **18:** 2479–2492.

Iwakawa, H., Ueno, Y., Semiarti, E., Onouchi, H., Kojima, S., Tsukaya, H., Hasebe, M., Soma, T., Ikezaki, M., Machida, C., and Machida, Y. (2002). The *ASYMMETRIC LEAVES2* gene of *Arabidopsis thaliana*, required for formation of a symmetric flat leaf lamina, encodes a member of a novel family of proteins characterized by cysteine repeats and a leucine zipper. Plant Cell Physiol. **43:** 467–478.

Izhaki, A., and Bowman, J.L. (2007). KANADI and class III HD-Zip gene families regulate embryo patterning and modulate auxin flow during embryogenesis in *Arabidopsis*. Plant Cell **19:** 498–508.

Jackson, D. (1992). In situ hybridization in plants. In Molecular Plant Pathology: A Practical Approach, D.J. Bowles, S.J. Gurr, and R. McPherson, eds (Oxford, UK: Oxford University Press), pp. 163–174.

Jun, J.H., Ha, C.M., and Nam, H.G. (2002). Involvement of the *VEP1* gene in vascular strand development in *Arabidopsis thaliana*. Plant Cell Physiol. **43:** 323–330.

Kerstetter, R.A., Bollman, K., Taylor, R.A., Bomblies, K., and Poethig, R.S. (2001). KANADI regulates organ polarity in Arabidopsis. Nature **411:** 706–709.

Kim, J., Jung, J.-H., Reyes, J.L., Kim, Y.-S., Kim, S.-Y., Chung, K.-S., Kim, J.A., Lee, M., Lee, Y., Kim, V.N., Chua, N.H., and Park, C.M. (2005). MicroRNA cleavage of *ATHB15* mRNA regulates vascular development in Arabidopsis inflorescence stems. Plant J. **42:** 84–94.

Li, H., Xu, L., Wang, H., Yuan, Z., Cao, X., Yang, Z., Zhang, D., and Huang, H. (2005). The putative RNA-dependent RNA polymerase *RDR6* acts synergistically with *ASYMMETRIC LEAVES1* and *2* to

repress *BREVIPEDICELLUS* and microRNA165/166 in Arabidopsis leaf development. Plant Cell **17:** 2157–2171.

Lin, W., Shuai, B., and Springer, P.S. (2003). The Arabidopsis *LATERAL ORGAN BOUNDARIES*-domain gene *ASYMMETRIC LEAVES2* functions in the repression of *KNOX* gene expression and adaxial-abaxial patterning. Plant Cell **15:** 2241–2252.

McConnell, J.R., and Barton, M.K. (1998). Leaf polarity and meristem formation in Arabidopsis. Development **125:** 2935–2942.

McConnell, J.R., Emery, J., Eshed, Y., Bao, N., Bowman, J.L., and Barton, M.K. (2001). Role of *PHABULOSA* and *PHAVOLUTA* in determining radial patterning in shoots. Nature **411:** 709–713.

Nakazawa, M., Ichikawa, T., Ishikawa, A., Kobayashi, H., Tsuhara, Y., Kawashima, M., Suzuki, K., Muto, S., and Matsui, M. (2003). Activation tagging: A novel tool to dissect the functions of a gene family. Plant J. **34:** 741–750.

Navarro, C., Efremova, N., Golz, J.F., Rubiera, R., Kuckenberg, M., Castillo, R., Tietz, O., Saedler, H., and Schwarz-Sommer, Z. (2004). Molecular and genetic interactions between *STYLOSA* and *GRAMINIFOLIA* in the control of *Antirrhinum* vegetative and reproductive development. Development **131:** 3649–3659.

Norberg, M., Holmlund, M., and Nilsson, O. (2005). The *BLADE ON PETIOLE* genes act redundantly to control the growth and development of lateral organs. Development **132:** 2203–2213.

Ori, N., Eshed, Y., Chuck, G., Bowman, J.L., and Hake, S. (2000). Mechanisms that control *knox* gene expression in the *Arabidopsis* shoot. Development **127:** 5523–5532.

Prigge, M.J., Otsuga, D., Alonso, J.M., Ecker, J.R., Drews, G.N., and Clark, S.E. (2005). Class III homeodomain-leucine zipper gene family members have overlapping, antagonistic, and distinct roles in Arabidopsis development. Plant Cell **17:** 61–76.

Sawa, S., Watanabe, K., Goto, K., Kanaya, E., Morita, E.H., and Okada, K. (1999). *FILAMENTOUS FLOWER*, a meristem and organ identity gene of *Arabidopsis*, encodes a protein with a zinc finger and HMG-related domains. Genes Dev. **13:** 1079–1088.

Semiarti, E., Ueno, Y., Tsukaya, H., Iwakawa, H., Machida, C., and Machida, Y. (2001). The *ASYMMETRIC LEAVES2* gene of *Arabidopsis thaliana* regulates formation of a symmetric lamina, establishment of venation and repression of meristem-related homeobox genes in leaves. Development **128:** 1771–1783.

Serrano-Cartagena, J., Robles, P., Ponce, M.R., and Micol, J.L. (1999). Genetic analysis of leaf form mutants from the Arabidopsis Information Service collection. Mol. Gen. Genet. **261:** 725–739.

Shuai, B., Reynaga-Pena, C.G., and Springer, P.S. (2002). The *LATERAL ORGAN BOUNDARIES* gene defines a novel, plant-specific gene family. Plant Physiol. **129:** 747–761.

Siegfried, K.R., Eshed, Y., Baum, S.F., Otsuga, D., Drews, G.N., and Bowman, J.L. (1999). Members of the *YABBY* gene family specify abaxial cell fate in *Arabidopsis*. Development **126:** 4117–4128.

Sun, Y., Zhou, Q., Zhang, W., Fu, Y., and Huang, H. (2002). *ASYMMETRIC LEAVES1*, an *Arabidopsis* gene that is involved in the control of cell differentiation in leaves. Planta **214:** 694–702.

Tang, G., Reinhart, B.J., Bartel, D.P., and Zamore, P.D. (2003). A biochemical framework for RNA silencing in plants. Genes Dev. **17:** 49–63.

Timmermans, M.C.P., Hudson, A., Becraft, P.W., and Nelson, T. (1999). *ROUGH SHEATH2*: A Myb protein that represses *knox* homeobox genes in maize lateral organ primordia. Nature **284:** 151–153.

Tsiantis, M., Schneeburger, R., Golz, J.F., Freeling, M., and Langdale, J.A. (1999). The maize *rough sheath2* gene and leaf development programs in monocot and dicot plants. Nature **284:** 154–156.

Tsukaya, H., and Uchimiya, H. (1997). Genetic analyses of the formation of the serrated margin of leaf blades in *Arabidopsis:* Combination of a mutational analysis of leaf morphogenesis with the characterization of a specific marker gene expressed in hydathodes and stipules. Mol. Gen. Genet. **256:** 231–238.

Venglat, S.P., Dumonceaux, T., Rozwadowski, K., Parnell, L., Babic, V., Keller, W., Martienssen, R., Selvaraj, G., and Datla, R. (2002). The homeobox gene *BREVIPEDICELLUS* is a key regulator of inflorescence architecture in Arabidopsis. Proc. Natl. Acad. Sci. USA **99:** 4730–4735.

Waites, R., and Hudson, A. (1995). *phantastica*: A gene required for dorsoventrality of leaves in *Antirrhinum majus*. Development **121:** 2143–2154.

Waites, R., Selvadurai, H.R.N., Oliver, I.R., and Hudson, A. (1998). The *PHANTASTICA* gene encodes a MYB transcription factor involved in growth and dorsoventrality of lateral organs in *Antirrhinum*. Cell **93:** 779–789.

Williams, L., Grigg, S.P., Xie, M., Christensen, S., and Fletcher, J.C. (2005). Regulation of Arabidopsis shoot apical meristem and lateral organ formation by microRNA *miR166g* and its *AtHD-ZIP* target genes. Development **132:** 3657–3668.

Xu, L., Xu, Y., Dong, A., Sun, Y., Pi, L., Xu, Y., and Huang, H. (2003). Novel *as1* and *as2* defects in leaf adaxial-abaxial polarity reveal the requirement for *ASYMMETRIC LEAVES1* and *2* and *ERECTA* functions in specifying adaxial identity. Development **130:** 4097–4107.

Xu, L., Yang, L., Pi, L., Liu, Q., Ling, Q., Wang, H., Poethig, R.S., and Huang, H. (2006). Genetic interaction between the AS1-AS2 and RDR6-SGS3-AGO7 pathways for leaf morphogenesis. Plant Cell Physiol. **47:** 853–863.

Xu, Y., Sun, Y., Liang, W., and Huang, H. (2002). The *Arabidopsis AS2* gene encoding a predicted leucine-zipper protein is required for the leaf polarity formation. Acta Bot. Sin. **44:** 1194–1202.